EEG SOURCE LOCALIZATION IN AN ECONOMIC MOTIVATION GAME

by

Mehmet Emin Kazanç

B.S., Electronics Engineering, Kadir Has University, 2015

Submitted to the Institute for Graduate Studies in
Science and Engineering in partial fulfillment of
the requirements for the degree of
Master of Science

Graduate Program in Electrical and Electronics Engineering
Boğaziçi University

2018

ACKNOWLEDGEMENTS

Firstly, I would like to express my sincere and greatest graditude to my thesis supervisors Prof. Yasemin P. Kahya and Prof. Burak Güçlü for crucial support during my thesis study. Their advices helped me to overcome this long journey. Their advices are very beneficial to complete this thesis and it has been an honor for me to be their master student.

I also would like to thank Prof. Emin Anarım, Prof. Murat Saraçlar and Assist. Prof. Mustafa Zahid Yıldız for accepting to be committee member.

I am very happy for being member of BULAL and BUSIM laboratories. I would like to thank all the members of those labs for their friendship.

Finally, my deepest thanks go to my family, especially my sweet sister and dear mother, grandmother and grandfather for their love and support. In addition, advices of my father was so important to finalize my thesis. I would not be able to write this thesis without their motivation and encouragement.

ABSTRACT

EEG SOURCE LOCALIZATION IN AN ECONOMIC MOTIVATION GAME

In this study, the correlations between EEG sources in multiple brain areas and the performance feedback in a motivation game were studied. EEG data were collected from 14 (6 male, 8 female) participants with 19 channels according to the standard 10-20 system. The task consisted of solving as many questions as possible in a given time-limited (2 min.) round. The questions were simple arithmetic, symbolic, and verbal items from typical IQ tests and displayed on the computer screen. Each participant competed with 10 human opponents for two rounds each, based on the responses collected from the opponents before the EEG experiments. After the first round against each opponent, the participant was given a text feedback ("You win!", "You lose!", or "It's a tie!"), depending on his/her score when compared to the opponent's score. Next, the participant was allowed to compete with the same opponent in a second round. After band-pass filtering, the artifactual components were identified by ICA and eliminated. Based on reconstructed EEG signals, dipole sources were localized by using EEGLAB and the standard boundary-element model. Multiple regression analyses were performed with total normalized moment magnitudes in different brain areas as the independent variables. Dependent variables were performance changes such as the net score change in the second round with respect to the first round, the change in the attempted questions, and the change in only correct answers. The results show that when positive feedback ("You win!") was given, the associative visual cortex, orbitofrontal area and ventral anterior cingulate cortex became significantly correlated with net score changes and the changes in the correct answers. On the other hand, when negative feedback ("You lose!") was given, dorsolateral prefrontal cortex and dorsal anterior cingulate cortex were significantly correlated with the same performance changes. Additional areas were also found in different rounds.

ÖZET

BİR EKONOMİK MOTİVASYON OYUNUNDA EEG KAYNAKLARININ BELİRLENMESİ

Bu çalışmada, bir motivasyon oyununda oluşan çoklu beyin bölgelerindeki EEG kaynakları ve performans geribildirimi arasındaki korelasyonlar incelenmiştir. EEG verileri 14 (6 erkek, 8 kadın) katılımcıdan 19 kanalla 10-20 sistemine göre toplanmıştır. Görev, belirli bir zaman sınırı içinde (2 dk.) ilgili turda mümkün olduğunca çok soru çözmekten oluşmaktadır. Sorular tipik IQ testlerinden basit aritmetik, sembolik ve sözel öğelerdir ve bilgisayar ekranında gösterilmişlerdir. Her katılımcı, EEG deneylerinden önce elde edilen rakiplerin cevaplarına dayanarak, her biri iki tur için 10 rakiple yarışmıştır. Her bir rakibe karşı ilk turdan sonra, katılımcıya kendi puanının rakibinden daha yüksek veya düşük olduğuna bağlı olarak ekranda bir metin geri bildirimi ("Kazandınız!", "Kaybettiniz!" Veya "Berabere!") verilmiştir. Ardından, katılımcı ikinci bir turda aynı rakiple yarışmıştır. Bant geçiren filtrelemeden sonra, artifaktlı bileşenler BBA ile tanımlanmış ve elenmiştir. Yeniden oluşturulan EEG sinyallerine dayanarak, dipol kaynakları EEGLAB ve standart sınır eleman modeli kullanılarak bulunmuştur. İstatistiksel olarak, bağımsız değişkenlerin farklı beyin alanlarındaki toplam normalize moment genlikleri ile çoklu regresyon analizleri yapılmıştır. Bağımlı değişkenler olarak, birinci turdan ikinci tura net skor değişimi, denenen soru sayısındaki değişim ve sadece doğru cevap sayısındaki değişim kullanılmıştır. Olumlu geribildirim ("Kazandınız!") verildiğinde, ilişkisel görsel korteks, orbitofrontal alan ve ventral anterior singulat korteksin net skor değişiklikleri ve doğru cevap sayısındaki değişiklikler ile anlamlı ve ilişkili olduğu bulunmuştur. Öte yandan, olumsuz geribildirim ("Kaybettiniz!") verildiğinde, dorsolateral prefrontal korteks ve dorsal anterior singulat korteks aynı performans değişiklikleri ile anlamlı olarak ilişkili bulunmuştur. Farklı turlar için de ilave alanlar da bulunmuştur.

TABLE OF CONTENTS

LIST OF FIGURES

LIST OF TABLES

LIST OF SYMBOLS

a_{ij}	Random Mixing Coefficients
B	Propagation Effect
C	Baseline Effect
C	Conductor Matrix
e_k	Position of Electrode
$E\{\}$	Expected value
fa	Frontal Asymmetry
n	Zero mean addictive gaussian noise
o	Orientation of Dipole
P(w)	Power Spectrum of data
r	3D location of dipole
U	Recorded Potential at scalp
X	Time Series Signal
$\overline{X}$	Mean of vector X

LIST OF ACRONYMS/ABBREVIATIONS

2D	Two Dimensional
3D	Three Dimensional
EEG	Electroencephalography
fMRI	Functional Magnetic Resonance Imaging
fNIRS	Functional Near-Infrared Spectroscopy
PET	Positron Emission Tomography
BOLD	Blood-oxygen-level Dependent
ACC	Anterior Cingulate Cortex
VMPFC	Ventromedial Prefrontal Cortex
PFC	Prefrontal Cortex
OFC	Orbitofrontal Cortex
ERP	Event-Related Potential
ICA	Independent Component Analysis
IMF	Intrinsic Mode Functions
EMD	Empirical Mode Decomposition
IC	Independent Component
MNI	Montreal Neurological Institute
SHM	Spherical Head Model
RV	Residual Variance
PF	Positive Feedback
NF	Negative Feedback
AF	Adaptive Filter
dACC	Dorsal Anterior Cingulate Cortex
dlPFC	Dorsolateral Prefrontal Cortex
NAcc	Nucleus Accumbens
VTA	Ventral Tegmental Area
EOG	Electrooculographic
BEM	Boundary Element Model

RLS	Recursive Least Square

1. INTRODUCTION

1.1. Aim, Background and Motivation

Humans give important decisions to proceed their life and sources of these decisions are very important in terms of science. At this point, economists usually try to find a rational economic model to explain those decisions. Although these models satisfy some of behavioral actions, they can not explain all the decisions. Recently, a new field called neuroeconomics came out to provide explanation by analyzing biological processes. To understand these processes, brain imaging is one of the most commonly used methods to analyze correlations between brain activity and given decisions. Literature now is getting bigger and bigger with many neuroeconomics experiments of human behavior with the help of signal processing tools. One of the interesting topics in this field is to understand the effect of motivational feedback on human performance and brain. More specifically, the question examined in this type of this experiment is to examine the motivation of people while competing with others, how their performances change, and what their reactions are to positive / negative feedback. The motivational effects of competitive incentive systems, and especially the gender differences in this issue, is a commonly studied subject in the economics [6]. Motivation can be defined as transforming a goal to action. The feedback given in this action affects particular brain areas and subsequent future actions. In general, the relationship between feedback, motivation and neural responses will be investigated in this thesis. In the analysis, neural responses were based on dipoles located in Brodmann areas derived from EEG data. According to our knowledge, the technique used in this experiment is the first in the literature and will provide insight into the study of motivation in neuroeconomics. Literature usually includes ERP related studies in short-time recording environments and this analysis provides some active regions in the brain. Suggested technique can be implemented long-time recordings in neuroeconomics experiments. Moreover, temporal resolution of EEG can provide better source localization in terms of milliseconds when compared with fMRI. This is one advantage of EEG to observe brain dynamics immediately. In addition to technique, the purpose of the experiment is (1) to examine whether the feedback increases or decreases the performance, (2) to correlate the performance with brain activations in relation with feedback. This results provide will new insights into neuroeconomics field. Additionally, some previous studies suggest that power changes in EEG frontal channels may also provide information about motivation. To test this hypothesis, the power spectrum of alpha band in response to feedback type was also investigated.

1.2. Outcomes and Organization of the Thesis

In the first chapter, aim, background and motivation of the thesis were explained. In Chapter II, literature background in neuroeconomics and commonly used methods for signal processing and source localization were explained. In addition, suggested methods to model obtained EEG-dipole data were stated. In neuroeconomics part, initially neuroeconomics field was introduced and intersection points between this field and engineering were expressed. Finally, related experiments with results were discussed. In signal processing part, artifact removal step is first explained. In the literature, several methods are used for removal of ocular artifact: Croft's Regression based method, adaptive filtering, empirical mode decomposition and independent component analysis. In the following subsection, the source localization method was explained. Then, prediction modeling based on dipoles was given. To model them, multiple regression, frontal asymmetry and power spectrum methods were used. In Chapter III, the methods used in experiment and signal processing step are explained in detail. Chapter IV consists of behavioral results and source localization results. Behavioral results show test performances of subjects in term of net score, number of attempted questions and the number of correct answers. Next, results from intermediate signal processing steps such as artifact removal, source localization were given. Finally, multiple regression analysis were shown for correlations between the dipoles from different brain areas and performance change. In the final chapter, general conclusions were stated and results were discussed with respect to previous studies in literature. The next section includes limitations of this study. The weak and strong point of the used methods and models were evaluated.

2. LITERATURE BACKGROUND

2.1. Neuroeconomics

Neuroeconomics is an interdisciplinary field that brings together researchers from economics, psychology, and neuroscience, what have developed greatly in recent years. The general aim of neuro-economics studies is to understand the projections and resources of the economic decisions of the people so that researchers can shed light on the mechanisms that make decisions and preferences [7].

The resources are interpreted as biological effects that are active brain regions, neuron reactions, genes, blood pressure, hormonal changes... These metrics provide understanding of biological mechanisms of economics cognition processes. Moreover, economic decisions and cognitions consist of reward processing, preferences, expectation and anticipation, memory, valuation, rewarding system etc. [7–11].

Economics normally deals with classical assumptions such as rationality and dynamic consistency. On the other hand, neuroeconomics mostly seek to find biological effects and sources which cause decisions and preferences. Instead of classical view, biological effects associated with decisions are on the mile stone of neuroeconomics. It also provides an opportunity to test and explain available theories related to choices with the help of neural data.

It is obvious that most important reactions occur in the brain. Scientists that study neuroeconomics use different imaging methods to find sources in the brain. EEG, fMRI, fNIRS and PET are common methods for brain imaging. Researchers can use this methods during economic activities like used problem-solving, multiple choice, time estimation tasks, decision-making, valuation etc. that belong to an economic activity. Functional magnetic resonance imaging (fMRI) is the most commonly used technique in neuroeconomics due to higher spatial resolution. However, it shows BOLD (blood-oxygen level) in the brain instead of neural activity directly. Increased neural activity causes the blood flow to increase as well as the oxygenated hemoglobin's density so that activations can be followed. Also, the location of these changes in the brain give clues in terms of functionality. For example: It was found that higher activation of right Anterior Insula caused subjects to reject unfair offers and authors inferenced that activations in this region may be related to the degree of emotion for unfair offers [12]. More detailed results will be explained in the following paragraphs of this section.

On the other hand, a disadvantage of fMRI is that it is "slow" in terms of time, in other words it can not distinguish short-lived changes. BOLD signals transmit activity in a delayed manner, appear firstly after 2 seconds. In this respect EEG is more advantageous and there are studies showing that EEG can be used successfully in neuroeconomics and can give similar results to fMRI [13].

Contextually, neuroeconomics studies do cover many topics. The most important of these are economic decisions made under risk and uncertainty, time preferences, and decisions regarding auto-control, alternative and just distribution [3, 12, 14]. Below paragraphs will exhibit neuroeconomic studies' processes and results related to particular domains.

The first topic is related to decisions under risk conditions. De Martino *et.al.* conducted a study to learn differences of neural activity corresponding of sure and risky choices with gain-loss outcomes. In other words, they tried to learn biological foundations of "Framing Effect" by using fMRI imaging method. Framing effect is presenting way of options by showing difference aspects. The subjects (20 students/graduates from university) needed to choose two options "Sure" or "Gambling" displayed as two different frames on the screen. Below figure 2.1 shows screen of the experiment steps. The same structure was displayed as two different ways (i.e. framing effect). It was obvious that expected outcomes of two choices were equal but more interestingly, subjects performed significantly different behaviors. They mostly tend to choose sure option in "Gain Frame" by staying away from risk and gamble option in "Loss Frame" by staying close to risk.

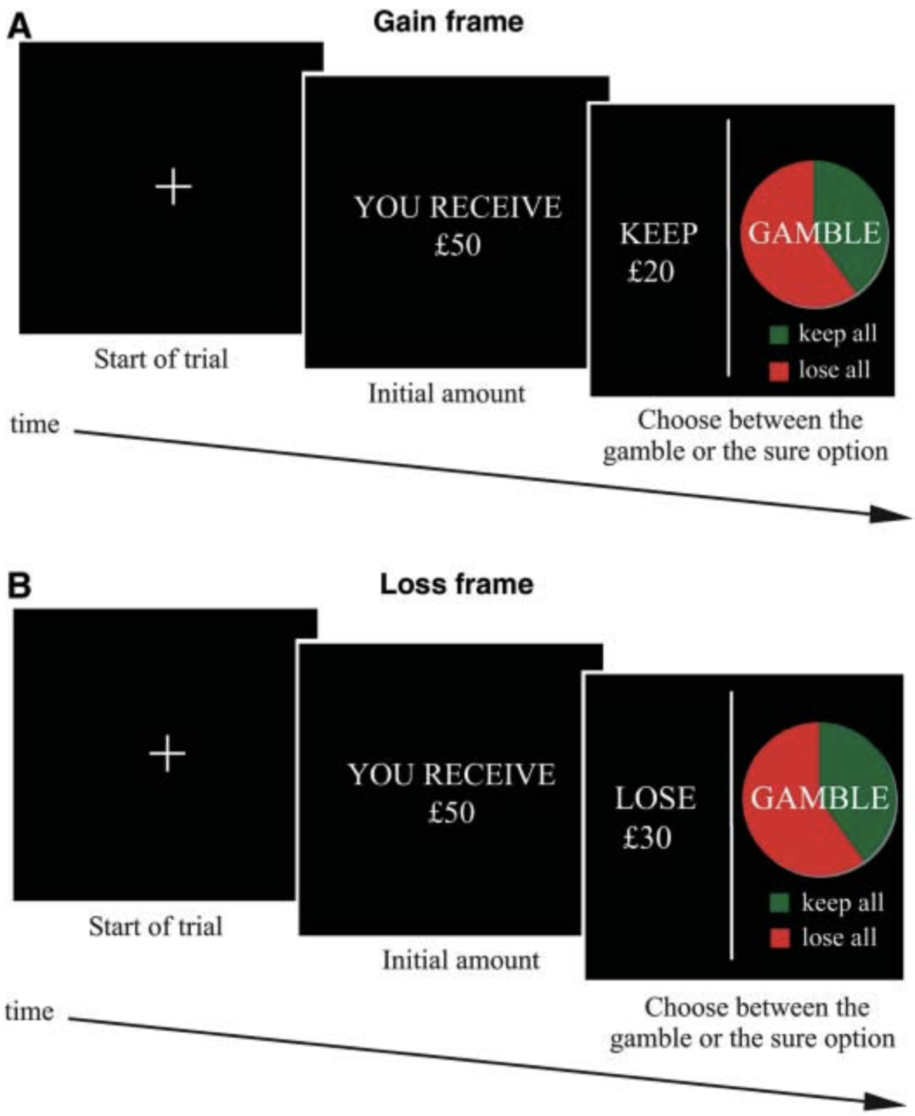

Figure 2.1. Financial Decision Making Task [1]

Biological processes were recorded in a fMRI scanner during experiment. Authors stated that framing effect was G_{sure} and L_{gamble} and counter part of the general behavioral tendency was G_{gamble} and L_{sure}. To learn behavioral tendency, authors looked at contrast by deriving this formula: $[G_{sure} + L_{gamble}]$ - $[G_{gamble} + L_{sure}]$ and according to results, they found activation in bilateral amygdala. To test this issue's consistency for both cases (Gain and Loss Frames), the same contrast difference was done between gain frame $[G_{sure}$ - $G_{gamble}]$ and loss frame $[L_{gamble}$ - $L_{sure}]$ separately. Moreover, it was again found significantly greater activations amygdala when subjects decided to choose the sure option in the gain frame and gamble option in loss frame. Another interesting analysis was completed by regarding counter part of general tendency. To understand

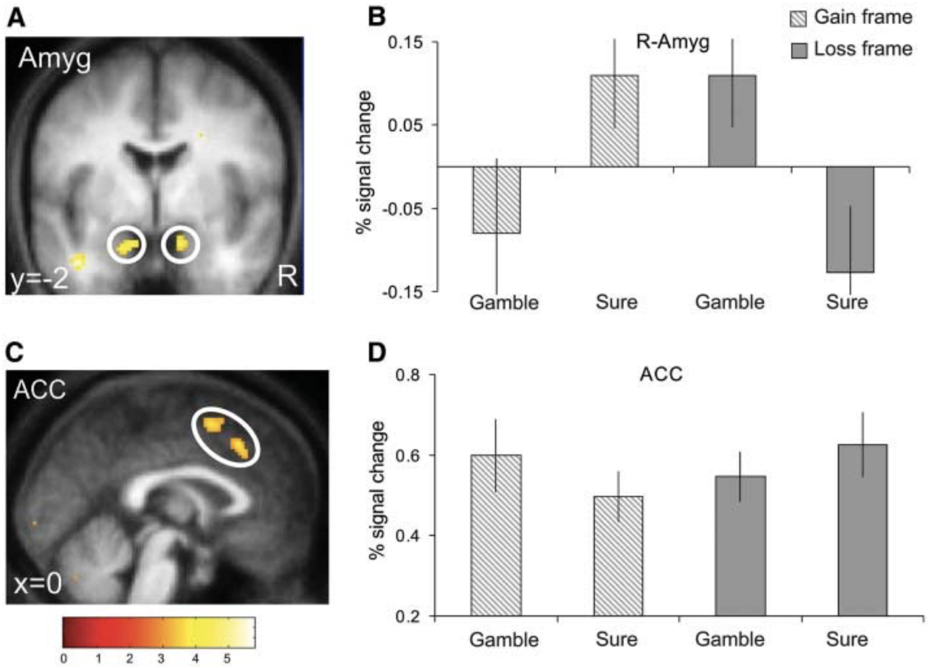

Figure 2.2. Biological Outcomes of Risky Decisions [1]

this effect, this formula was derived $[G_{gamble} + L_{sure}]$- $[G_{sure} + L_{gamble}]$. When subjects choose gamble option in gain frame and sure option in loss frame, above derived formula comes out some contrasts. They observed increased activity in the anterior cingulate cortex(ACC). When those activations were interpreted in term of functionality, amygdala was related to subject's risk-averse behavior in Gain Frame and risk seeking behavior in Loss Frame. This was called Framing Effect by authors. Then, it was stated that this framing effect was driven by systems related to emotionality and amygdala plays crucial role in value-prediction learning for both positive and negative outcomes. In addition, subjects behaviour related to counter part of general tendency caused activation in ACC. It was also stated that this activation may be due to conflict between emotional and analytic responsive systems in the brain [1, 15, 16].

Another phenomenon in decision-making under risk is loss aversion behavior. Tom *et.al.* conducted a study to clarify this issue by looking neural basis in the brain. The authors referenced Prospect Theory to explain this concept. This theory says that humans become much more sensitive when they have lost money or any other objects by comparing gaining correspond object or money. They generally want to be offered gaining as twice of loss. In other words, potential gain amount must be twice of the potential loss to be tolerable for humans [17–19].

People are more sensitive to the possibility of losing objects or money than they are to the possibility of gaining the same objects or amounts of money. Thus, people typically require a potential gain of at least $100 to make up for exposure to a potential loss of $50 because the subjective impact of losses is roughly twice that of gains. In this study, utility of decision was evaluated by the help of fMRI method. Previous studies investigated anticipated and experienced utility but this study was based on decision utility [2, 20–23].

One of the main questions in this study is to learn loss aversion causes of emotional effects when potential losses are evaluated. There are some studies in the literature which conclude fear-anxiety may drive sensitivity level for potential losses [24]. In addition, authors searched which region in the brain loss aversion activates regarding responses to gains-losses. Subjects were asked to accept or reject two options (50/50 chance) to gain or loss offered amounts. This system was shown in the following figure 2.3. A shows matrix of offered choices, B shows probability of acceptance and C displays response time. In B part, it can be easily understood that red means that much more willingness and blue means that much more reject probability of offer.

As a result, potential gain increment caused activations in the midbrain dopaminergic areas. Specifically, dorsal and ventral striatum, VMPFC, ventro-lateral PFC, anterior cingulate cortex (ACC), OFC become more active and this may be associated with monetary awards and anticipation. However, losses caused decreased activity in some of the same regions of potential gains such as striatum, VMPFC, ventral ACC, and medial OFC instead of activations in different fields of the brain. These results were shown in figure 2.4.

More interestingly, authors concluded that there was a joint sensitivity for potential gains and losses. In addition, the worst and best possible result of gambles were compared and activations were evaluated. By the way, the best coded as gain: $34 to $40; loss: $5 to $8 and the worst coded as gain: $10 to $16; loss: $17 to

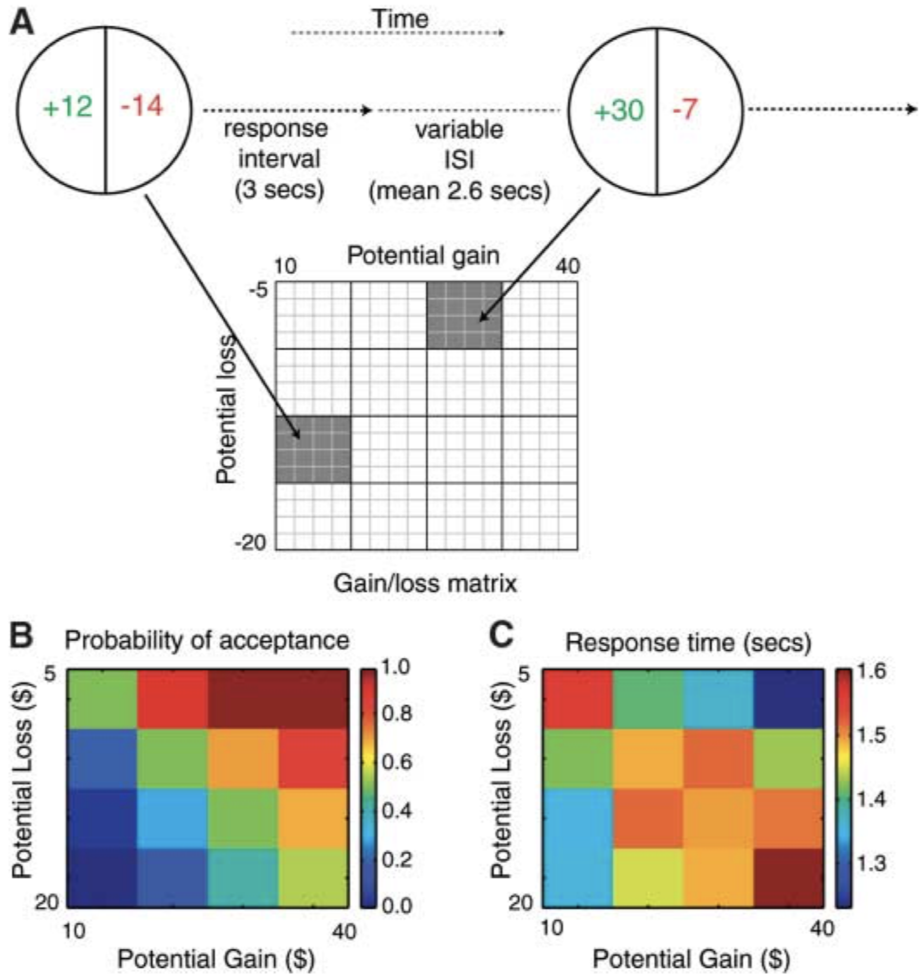

Figure 2.3. Event-Related Potential Gain-Loss Game Design [2]

$20. Although there was no more significant activation for worst cases, the ventral striatum and VMPFC become more active for the best possible gambles. All in all, authors said that potential loss and gains were driven by the same mechanism instead of two distinct systems. This result was attributed to previous studies that mention increased and decreased activity of striatum in case of experiencing monetary gain and loss situation [21, 22]. Lastly, one of the unique results of this study was that anticipated/experienced losses may activate regions that may be associated with negative emotions like amygdala, anterior insula according to literature. Conversely, this study concluded that potential losses were coded in decreased activity in regions of potential gains instead of different regions like previous studies results. This difference in results shed light on importance of experienced, anticipated and decision utility choice theories in economics [25, 26].

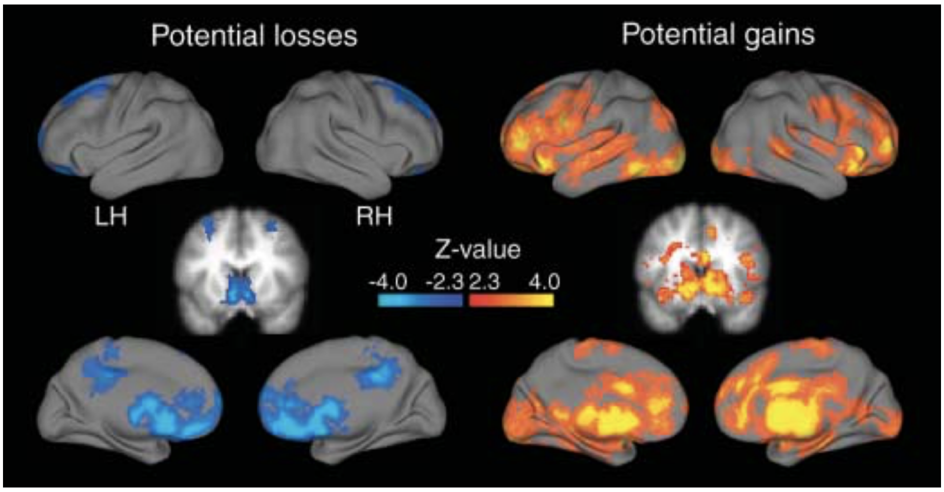

Figure 2.4. fMRI Results of Potential Gains and Losses [2]

Another hot topic in this area is inter-temporal choice. People were offered two choices like given 10$ immediately or 11$ tomorrow. They behave differently for this selection process. At this point, McClure *et.al.* conducted a study to seek neural correlates of preferences between immediate and delayed choices. According to their hypothesis, short-term decisions were driven by limbic system and long-term decisions were driven by prefrontal cortex and associated structures. In the literature, there was a model that explains time-discounting function and it was proposed by Phelps and Pollack [27]. They stated this model in the formula given below. β is coefficient for delayed rewards received in time, δ is discount rate and u is reward value at t=0.

$$\text{Reward Value} = \begin{cases} u, & \text{if } t = 0 \\ \beta\delta^t u, & \text{if } t > 0 \text{ where } 0 < \beta \leq 1 \text{ and } \delta \leq 1 \end{cases} \tag{2.1}$$

Subjects in this experiment made choices between early and later options such as immediately 10$ or two weeks later 12$. Moreover, earlier options were always lower than later options. Amounts were sorted from 5$ to 40$ and time were sorted from immediate to 6 weeks. fMRI recordings were received from subjects during experiment. The first analysis is to learn differences of choices for immediate reward (today $t = 0$)

and delayed rewards(later t≥ 0). As a result of this, areas of limbic structure consists of ventral striatum, medial orbitofrontal cortex, and medial prefrontal cortex become more active after immediate option was selected as expectedly. Below figure 2.3 shows that these areas become more active when $d = Today$ was selected when compared with later options.

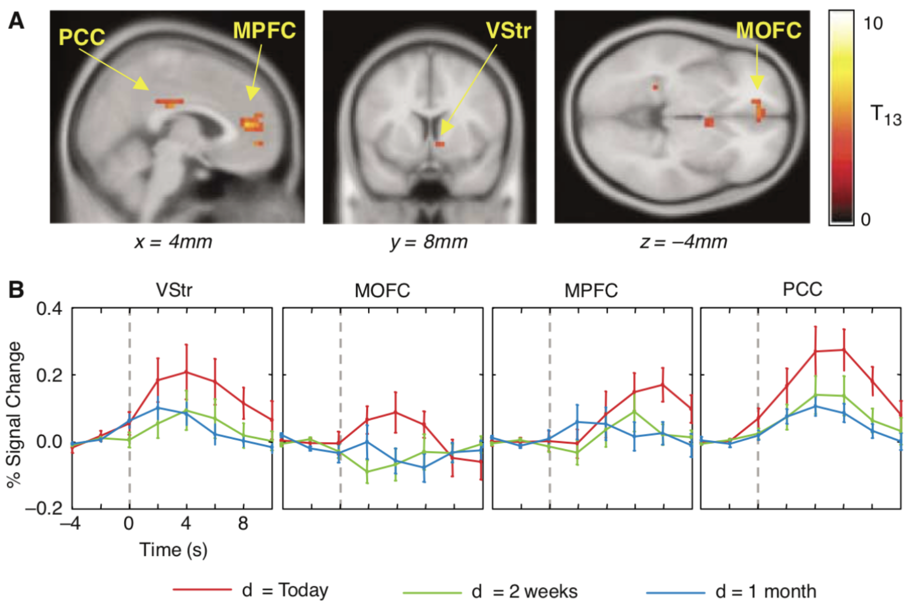

Figure 2.5. Active Structures After Immediate Option Selection [3]

In addition, there were some active areas in all decisions epochs that do not depend on preference. Those were visual processing and motor-response areas, not related task performance. Moreover, difficulty of decision making by adjusting difference of two offered options caused significant results in prefrontal and parietal cortex. Activations in those areas can be interpreted as consistent with studies in literature in terms of high-level cognitive functioning [16, 28].

fMRI is commonly used method for brain imaging in neuroeconomics experiments due to spatial resolution, which means that location of activations are much more reliable than other methods. Until now, fMRI related studies have been summarized. An alternative to fMRI in terms of cost and temporal resolution is EEG. It shows brain dynamics in miliseconds and this provides researchers to see immediate changes. In the following part, EEG based neuroeconomics studies are evaluated.

One of the most common methods is using EEG is identifying Event Related Potentials (ERPs) after given stimuli. Then, ERP's amplitude or localization are used to attribute neural correlates of stimuli. For example; there is a study to look at the result of the monetary gambling game. As a result of this study, such a meaningful outcome (P300-slow-wave component outcome) came out and it was concluded that relationship between polarity, latency and amplitude of this component with the amount of money that has been gained or lost become correlated [29–31]. Regarding this concept, Sanfey *et.al.* conducted a study to understand relationship between Event Related Potential(ERP) of response of offered reward and subject's behaviors. It was asked whether larger-smaller gain or lost affects P300 amplitude. The figure 2.6 below shows experimental design.

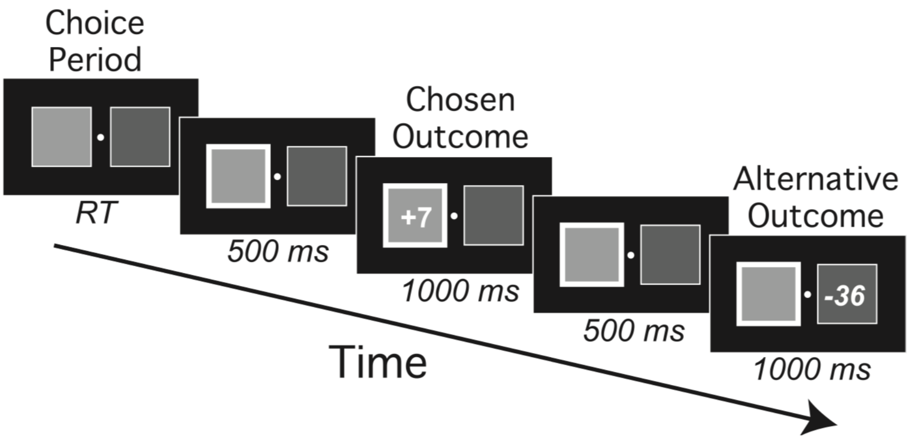

Figure 2.6. Gambling game design - Displaying Options [4]

In the following figure 2.7, feedback related ERP was characterized by P300 structure that was peaking after feedback was shown. Magnitude and valence of the chosen outcome caused different results.

Another aspect is to learn scalp topography response between valence and magnitude of selected options 300 miliseconds after stimuli presentation. According to results of [large - small] outcomes for both wins and losses, P300 amplitude becomes greater than at posterior midline sites that corresponds to Cpz and Pz channels. However, this amplitude reduced at frontal and lateral electrode positions. In addition, feedback related negativity (base to peak voltage difference 200-400 miliseconds after stimulus)

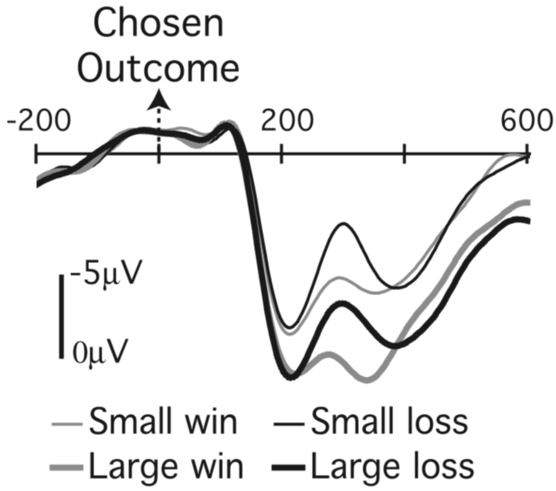

Figure 2.7. EPR results for 4 different stimuli [4]

was evaluated and concluded that it was greater after losses than gains.

Until now neuroeconomics theory by introducing some milestone topic's experiment was explained. In this experiment, subjects were given feedback to change their motivation and neural response to this given feedback was investigated. Motivation also played important role in this field. Now, in the following paragraphs related studies will be explained.

The first study was done to find the relationship between motivation and reward [32]. It was stated that mesolimbic and mesocortical regions such as Nucleus Accumbens(NAcc), VTA(Ventral Tegmental Area) and dlPFC(dorsolateral prefrontal cortex) interactions related to motivated behaviors and influence of motivation to these regions were investigated in this study. They concluded that potential reward information enters and activates dlPFC and this region transmits this information to other mesolimbic and mesocortical dopamine systems. Common points between this study and thesis focus can be stated as: after reward was given instead of any feedback, subjects behaved with different motivational situation. fMRI recording was done after reward was presented and before execution of motivated behavior to seek motivational activations.

In literature, there was another important study whose results related to dACC. They concluded that this area is responsible from detecting target such as detection of error or monitoring performance, evaluating rewards and influence motor responses. Bush *et.al.* conducted a study to shed light on this issue. They concluded that when subjects were shown reduced amount of reward, a strong activation in dACC region was found [33]. Furthermore, performance monitoring and competition monitoring capability of this region was also evaluated in the following studies [34–36].

2.2. Artifact Removal

Artifacts are one of the most challenging parts of EEG signals. When we look at the literature, we can list different kinds of artifacts. Those are eye blinks, horizontal eye movements, vertical eye movements, muscle movements, generic discontinuities, line noise... To clean those artifacts, a lot of methods were suggested such as blind source separation, adaptive filtering, wavelet filtering, empirical mode decomposition, canonical correlation analysis... [37–43]. Each method focuses on different aspects of artifact removal such as time domain, frequency domain analysis or spatial information. Recorded EEG data in this experiment are highly contaminated with ocular artifacts. Suggested methods that are convenient for ocular artifact removal were used in this thesis.

When we analyzed our signals, eye blink and movements were the most corruptive part of signals that's why it was needed to be got rid of eye-related artifacts. In literature, regression based methods, ICA and adaptive filtering were used to overcome this problem. These three methods were implemented and performance results were compared to select the most appropriate method.

2.2.1. Croft's Regression Method

Ocular artifacts are eliminated by using this method but there needs to be taken a calibration section after or before the real experiment to obtain particular correction coefficients for subjects. This calibration section includes eye movement trials by looking vertically, horizontally and radially in random way. After that, subject's eye movement coefficients are obtained for each movement type. Below formula shows how to find coefficients. B can be stated as propagation effect's coefficient and C can also stated baseline effect [44].

$$B = \sum(X_i - \overline{X}_i)(Y_i - \overline{Y}_i)/\sum(X_i - \overline{X}_i)^2 \tag{2.2}$$

$$C = \overline{X}_i - (\overline{Y}_i.B) \tag{2.3}$$

Above formulas show relation between EOG and EEG channels. X_i is EOG channel, Y_i is EEG channels and i is time instant. After B and C are obtained by calibration section, they are used for artifact correction. Following lines show how this is to be done. $estTEEG$ is the estimated value after correction, $MEEG$ is measured voltages at one of channels.

$$estTEEG_i = MEEG_i - (B.EOG_i) - C \tag{2.4}$$

2.2.2. Adaptive Filtering

Adaptive filtering is another suggested method for ocular artifact removal. Simultaneous EEG and EOG recordings satisfy adaptive filtering requirements. EOG channels are multiplied by some determined coefficients and then result is subtracted from EEG channels to obtain cleaned signals. In the suggested method, RLS (Recursive Least Square) filtering was used due to some advantages such as stability and rapid convergence. Below figure 2.8, used structure for adaptive filtering is shown [5].

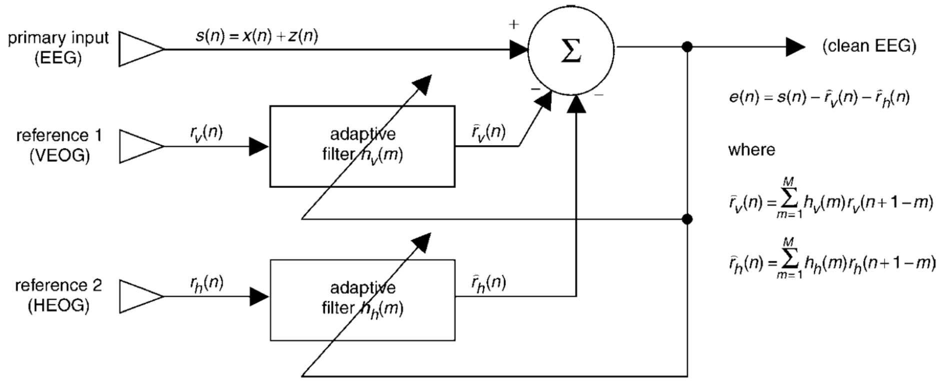

Figure 2.8. Block Diagram of EOG Noise canceler [5]

As the diagram displays, at each time n, desired original signal was updated by adjusting filter coefficients regarding error minimization and using EOG reference channels. Filter coefficients were obtained by correlation matrices of EOG reference channels and EEG-EOG correlation matrices. R is EOG correlation matrices, H is filter coefficients and P is EEG-EOG correlation matrices. After filter coefficients are found, vertical and horizontal movement effects are eliminated according to stated formula in the figure 2.8. Basic operations to find filter coefficients are shown in the following formulas.

$$R = \begin{bmatrix} R_{vv} & R_{vh} \\ R_{hv} & R_{hh} \end{bmatrix}$$

$$H = \begin{bmatrix} H_v \\ H_h \end{bmatrix} P = \begin{bmatrix} P_v \\ P_h \end{bmatrix}$$

$$RH = P \tag{2.5}$$

$$H = R^{-1}P \tag{2.6}$$

2.2.3. Independent Component Analysis

Independent Component Analysis or shortly ICA, is a blind source separation method used to find statistically independent sources. There is a classical example to explain its concept that is called cocktail-party problem. Assume that; there are a lot people in a room and equal number of microphones that are located at different fields. When someone from outside listens to one of the speakers, s/he hears mixed voices. Then, the question arises like "How can those microphone recordings are separated as one person's speech?". ICA plays crucial role for solution of this problem. This method basically finds statistically independent sources when those sources were linearly mixed and non-gaussian variables. ICA firstly subtracts mean from the signal and decorrelation step comes. It whitens data and then tries finding the most ideal weight matrix to obtain maximum non-gaussianity through related metrics like Negentrophy or Kurtosis [45, 46]. In addition, there were lots of ICA algorithms such as fastICA, Infomax, Extended-Infomax algorithms.

$$x_1(t) = w_{11}s_1(t) + w_{12}s_2(t) + w_{13}s_3(t) \tag{2.7}$$

$$x_2(t) = w_{21}s_1(t) + w_{22}s_2(t) + w_{23}s_3(t) \tag{2.8}$$

$$x_3(t) = w_{31}s_1(t) + w_{32}s_2(t) + w_{33}s_3(t) \tag{2.9}$$

$$X = WS \tag{2.10}$$

Above equations show three sources and three observations procedure. Sources are s_1,s_2 and s_3 and the are linearly mixed with weight coefficients. There may be more than three sources up to N. For cocktail-party problem case, s_1,s_2 and s_3 are speech signals of three people in time series, w's are weights according to distance of microphones. After weight matrix was found, inverse of this matrix is multiplied with recorded signals x to obtain independent sources can be obtained. From EEG-MEG-ICA... point of view, sources are neurons' activities in the brain.

Moreover, Makeig *et.al.* evaluates EEG and ICA relation in three different ways. Firstly, EEG signals are mixed with neural sources and artifactual sources in the linear environment. Also, time delays are negligible due to instantaneous and linear volume conduction. In addition, EEG activity is time locked but other artifactual sources like eye movement and muscle activity, line noise, cardiac signals are not time locked. The last statement points to the number of sources. It is a little bit questionable because ICA separates recorded signals as number of recorded sensors but there may be more than N sources. As a result of previous statements, mixing medium, negligible time delays and independence satisfies requirements of ICA implementation in EEG signals. The only problem may be related to the number of sources assumption. However, many simulation results suggest that ICA can find independent time activities and scalp topographies properly even in the extreme cases.

As stated before, there are two crucial steps for ICA. These are mean averaging and whitening. Mean averaging is simple subtract mean from the signal to get zero mean. Whitening is a process that decorrelates signal so that covariance matrix will be identity. Then, ICA becomes ready to find weight matrix W. Operations were shown as mathematical notations.

$$x = x' - E\{x'\} \tag{2.11}$$

$$E\{zz^T\} = I \tag{2.12}$$

$$z = Vx \tag{2.13}$$

$$C_x = EDE^T \tag{2.14}$$

Firstly, whitening means that covariance matrix is identity. Above formula Vx operation was called whitening transformation. To find this V value, eigenvalue decomposition of C_x was a suggested method in the literature. In the last formula above, E is orthogonal matrix that satisfy $E^T E = EE^T = I$ and finally covariance of z was calculated and identity matrix was found. According to this decomposition, V was found using the formula below.

$$E\{zz^T\} = VE\{xx^T\}V^T = D^{-1/2}E^TEDE^TED^{-1/2} = I \tag{2.15}$$

$$V = D^{-1/2}E^T \tag{2.16}$$

After finding W matrix, sources are found. Then, artifactual sources must be extracted by making them zero and recorded signals were reconstructed. Finally, artifact-free signals were obtained. To specify artifactual sources, kurtosis, time series correlation, power spectral density correlation, entropy, slope of power spectrum, low autocorrelation, focal channel topography are suggested methods for different artifact types [47, 48]. All in all, ICA was found so beneficial in terms of convenience of assumptions of EEG. Today, artifact removal and source localization processes are commonly used with ICA in EEG signal processing literature.

Another important issue is using optimal ICA algorithms. In literature, fastICA, Bell-Sejnowski Algorithm, Infomax, Extended-Infomax and JADE were commonly used methods. Although ICA algorithms were different from numerical point of view, their theory is similar. fastICA algorithm basically maximizes the absolute value of kurtosis metric. On the other hand, Bell-Sejnowski uses negentrophy value for separation of sources. Extended-Infomax minimize mutual information project axes and its advantage is separation of sources even if they have negative kurtosis value. Also, JADE maximize kurtosis probability density function [45, 49].

2.2.4. Empirical Mode Decomposition

EMD is a decomposition method for time series signal. It basically separates signal into intrinsic mode functions (IMFs) by using local maximum and local minimum points. IMFs are oscillating waveforms that are obtained by implementing two steps [50, 51].

$$x(t) = \sum_{i=1}^{n} [imf_i + n(t)] \tag{2.17}$$

The number of IMF extrema (the sum of the maxima and minima) and the number of zero-crossings must either be equal or differ at most by one

Those steps are (i) number of zero crossings of IMF should be equal or maximum one difference to extrema points. (ii) The other one is that mean of generated envelopes from maxima and minima points must be zero. Decomposition goes until the $n(t)$ become a monotonic function. After required metrics were satisfied, imf's are obtained and they are basically sorted according to frequency values from higher to lower.

Although this method provides some solutions in the literature, it also has negative disadvantages because of sensitivity of noise. The problem is called mode mixing effect. After imfs are obtained, it is concluded that each component has their particular frequency but noise may not have the same frequency values and may be located to different components of imf's. To solve this problem, EEMD algorithm is suggested [51]. This algorithm performs the operation as well as ensemble number and then take average of them to extract noise effect. By the way, this process is called noise assisted data analysis. After averaging imf's, noise could be eliminated. Finally, artifactual components are selected in decomposed components set. Then, artifactual ones are eliminated and remaining components are used to reconstruct original signals.

2.3. Source Localization

Dipole sources in the brain cause potential difference on the scalp. EEG basically records those potential changes due to electrical activity of neurons. At this point, dipoles caused potential change is stated as forward problem. On the other hand, finding active sources by using recorded EEG signals is called inverse problem. Solving inverse problem does not generate unique solution so that there are many possibilities under additional assumptions.

DIPFIT is a widely accepted tool for source localization. In this experimental data analysis, this toolbox was used. It performs this operation by using non-linear optimization technique by employing head model. [52].

There are basically 5 steps for source localization.

(i) Independent component analysis is performed to find neural sources.
(ii) Channel locations are adjusted.
(iii) Head models are set as Boundary Element Model or Spherical Head Model.
   - BEM is used in this analysis due to it is more realistic model and provides more accurate results.
(iv) Grid Scanning is performed. This operation is beneficial for the following step because GS points out initial locations of dipoles in 3-D. After those locations are found, they are used for dipole fitting as possible locations.
(v) Non-linear Interactive Fitting is performed. It mainly runs optimization algorithm to seek best positions for each independent component. Optimization parameters are locations and strengths of dipoles in 3D.

2.3.1. Independent Component Analysis

The main concept of ICA was explained in the previous part. In addition, ICA is used to extract independent components and then each one is used to find dipoles in the brain. Source localization algorithm is run for each component respectively.

2.3.2. Head Models

In EEGLAB-DIPFIT package, there are two models which are Spherical Head Model and Boundary Element Model. The first model includes skin, skull, cortex, CSF and the second one BEM consists of skin, skull, cortex structures that are extracted from the MNI (Montreal Neurological Institute) canonical template brain. According to authors, BEM provides much more realistic and accurate results than four concentric spheres model. One of the disadvantages of this model is that it is a numerical model and may cause incorrect solutions due to instability of numerical calculations. On the other hand, spherical model is an analytical model.

2.3.3. Grid Search

Grid search provides suitable starting points for dipole fitting procedure. The grid search was done in 3-D. (-85,85,11) includes 10 steps that start from -85mm to +85mm for X and Y direction. In addition, (0,85,11) was default settings for Z direction because dipoles are more consistently interpreted on the cortex instead of white matter.

2.3.4. Dipole Fitting

The previous part provides possible initial points for dipole fitting. In this step, the most optimal dipoles are selected by looking at dipole strengths and locations. To do that, a non-linear optimization algorithm was performed [53, 54].

2.3.5. Talairach Coordinate Transform

DIPFIT results include dipole locations and moment magnitude information. Both are used for the next modeling part. Moreover, location information is important to learn corresponding Brodmann areas on the cortex. This transformation results in particular brain areas such as Premotor Cortex, Middle Temporal Gyrus, Dorsalateral Prefrontal Cortex etc [55, 56].

2.4. Modeling

2.4.1. Multiple Regression

Regression is used to understand casual relationship between processes. For example: number and longitude of coke advertisement may affect customers to buy coke or this concept can be implemented to smart phones sales. According to mathematical terms, this model can be stated below. Y is dependent variable, b_0 is intercept and b_1 is slope of the curve (i.e. one unit change in X cause b_1 unit change in Y) [57].

$$Y = b_0 + b_1 X \tag{2.18}$$

More generally, linear regression may not be enough to model with multiple variables. At this point, multiple regression provides us to seek relationship between several independent variables and dependent variable by using least-square procedure. For example; financial earning is a function of experience, level of education, age and job title. Multiple regression finds effects of each independent variable. This relation can be stated as mathematically below. n is number of independent variable, i is sample in time domain and b's are coefficient of independent variables.

$$Y_i = b_0 + b_1 X_{1i} + b_2 X_{2i} + b_3 X_{3i} + ... + b_n X_{ni} \tag{2.19}$$

In the experiment, Brodmann areas and their moment magnitudes were used as independent variables. On the other hand, performance change in terms of net score, number of attempted questions and number of correct answers are used as dependent variables.

2.4.2. Frontal Asymmetry

Frontal asymmetry is used in some scientific studies as metric of motivational and emotional responding of stimulus. In addition, there are some studies that state power difference between left-right at frontal channels reflects valuable information. For example: Coan *et.al.* found that higher activations in the left compared with right means positive feelings [58]. Another study found that frontal asymmetry of alpha band in power spectrum can be a biomarker to interpret processing of information in both positive and negative ways [59]. Moreover, more left to right activity at frontal channels give clues about motivation or emotion like joy. However, more right to left activations provide information about fear, sadness and withdrawal motivation [60].

To calculate value related to frontal asymmetry, F3 and F4 or F7 and F8 channels were used. Power was calculated in alpha bands (8-12 Hz). More significantly, signals were separated to 1.5 seconds with Hamming windows. After average power spectrum was obtained, alpha band power was calculated.

$$fa = log\frac{P(F4)}{P(F3)} \tag{2.20}$$

2.4.3. Power Spectrum

In addition to frontal asymmetry metric, there are some studies to explain motivation by looking at alpha and delta bands power spectrum. To learn whatever power changes or not, alpha, beta, delta and theta bands power were evaluated in those studies. [61–64]. All in all, frontal asymmetry and power spectrum were also used to model performance change similar with moment magnitude of Brodmann regions. Results will be explained in particular section.

3. METHODS

3.1. Subjects

Subjects were 14 university students, with 8 female and 6 male subjects. Their age range between 20-25. They are all university students and their age between 20-25. Opponents were another set of 10 people that had done this experiment without EEG recording.

3.2. Apparatus

EEG device was Sagura Medizintechnik GmbH, Mühlheim am Main Germany. 19 electrodes were located at scalp and remaining 7 electrodes were around eyes. These were placed according to 10-20 system. This recording was done in a sound and vibration proof environment. Electrodes that were used for recording were 19 gold-plated, 9-mm disk. Ear electrode was used as reference in EEG device.

3.3. Procedure

Subjects viewed task questions on the computer screen and responded by pressing keys. The task consisted of solving as many questions as possible in a given time-limited (2 min.) round. The questions were simple arithmetic, symbolic, and verbal items from typical IQ tests (Fig.3.1) and displayed on the computer screen. Sample questions were shown below. Each participant competed with 10 human opponents for two rounds each, based on the responses of the opponents obtained before the EEG experiments. After the first round against each opponent, the participant was given a text feedback ("You win!", "You lose!", or "It's a tie!"), depending on whether his/her score was higher, lower, or the same compared to the opponent's score. The score was calculated as the sum of correct answers minus one fourth of the sum of incorrect answers. Next, the participant was allowed to compete with the same opponent in a second round.

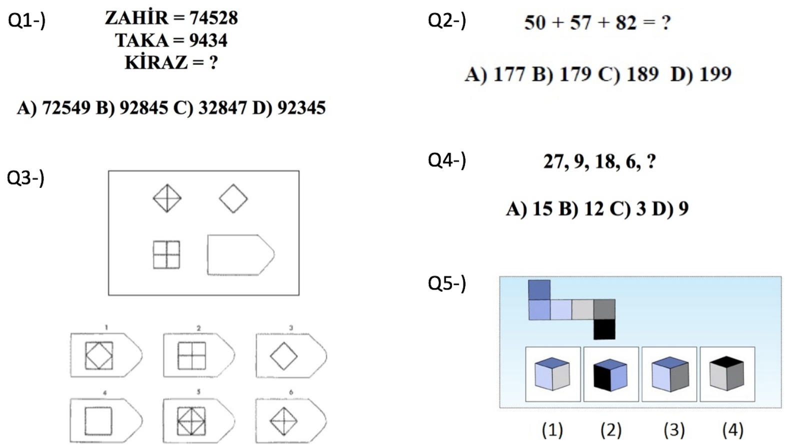

Figure 3.1. Sample Questions

The experiment performed by Prof.Güçlü at Institute of Biomedical Engineering at Boğaziçi University. Approvals were obtained from the ethics committees of Bogaziçi University. Recorded EEG data were first analyzed with signal processing tools to get rid of artifacts and then source localization algorithm was performed to find active dipoles in the brain.

3.4. EEG Preprocessing

3.4.1. Filtering

First, recorded EEG signals' mean was made zero for each channel. Then, each channel was band-pass filtered (1–70 Hz) with a zero-phase non-causal filter. To prevent phase shifting, filtering was done in forward and backward directions.

3.4.2. Artifact Removal

In the experiment, recorded EEG signals were mostly contaminated by ocular artifacts. To get rid of those artifactual parts, Croft's regression based method, adaptive filtering, ICA and EMD were performed respectively. After that, some metrics were used to evaluate for deciding on the most convenient one. Moreover, some channels that were effected badly due to measurement problems were also extracted before analysis.

Croft's method was explained in the introduction section. In calibration section, each subject had some coefficient that show of the relationship between EOG and EEG channels. Those coefficients were used to clean artifacts. This calibration section was performed after the experiment and it basically includes some pre-determined eye-movements that is shown to subjects on the screen.

Adaptive filtering had some similarity with Croft's method except calibration section. It finds correction coefficient by looking at the correlation between EOG and EEG channels. After EOG effects were extracted adaptively updating filter coefficients, EEG channels were cleaned.

ICA is one of the most popular methods for EEG artifact removal literature. It basically finds statistically independent sources by looking at non-gaussianity. After independent sources were obtained, selecting artifactual ones was a very crucial step. At this point, EOG channels played significant role. Correlation coefficients were found between each component and eye channels respectively. Lower eye channels and horizontal eye channels were used for correlation. At the end, each EEG channel had 4 correlation results associated with eye channels. Then, the average result was calculated. Another important step was choosing the threshold value. If correlation result was above threshold, it must be extracted as artifactual component. If threshold is above the correlation, those components were not extracted. In this system, threshold value was selected as 0.33 and all components were also evaluated visually to verify selected threshold's convenience. Although automatic selection is possible for threshold value by using some methods like Expectation-Maximization algorithm, visual verification of artifactual ICs provides to control performance of used method at the end. This threshold value can change with sampling rate, channel locations, duration time... More importantly, Extended-Infomax was chosen as ICA algorithm due to its high performance for source separation especially to determine artifactual sources.

Another selection criteria was based on variance. Ocular components variance generally become top 3 variance regarding whole components' variance so that 3 components that have the highest variance were selected as artifactual components.

Empirical mode decomposition was another source separation method in time domain. It was implemented directly for each channel but the problem was selection of intrinsic mode functions. IMF's were extracted and each channel then was reconstructed. Moreover, EMD may not work in noisy environment so that EEMD is the more developed version to overcome noise effect. After both algorithms were run, extracted IMFs were evaluated.

3.4.3. Performance Metric

Performance evaluation was done by comparing artifactual and non-artifactual segments' rms value. This was decided by using below formula. N was selected as 5 milliseconds. Whole recorded signal in a channel was separated into those 5ms segments. After that, rms value was calculated for each segment. At the end of this operation, the maximum and minimum 5 segments' rms values were saved to evaluate artifact removal performance. Maximum rms value segments were called artifactual segments and minimum rms value of 5 segments were called non-artifactual segments. Those segments were also verified visually. Then, average of 5 segments were taken to find a uniques rms value for particular group.

$$x_{rms} = \sqrt{\frac{1}{N}\sum_{n=1}^{N} x_n^2} \tag{3.1}$$

After artifact removal methods were implemented, corrected signals were examined by using this rms metric. Steps taken for performance comparison for one channel and person stated below. Then, performance comparison was shown in the results section.

- Calculate rms value of segments(5 ms) for Fp1 and Subject-1.
- Extract maximum and mininum 5 rms value and take mean.
- Do this operation for Fp1 channel before and after artifact removal.
- Then, perform similar operation for each trial and round.
- Next, give those 2 average rms lists(artifactual-nonartifactual) into ttest.
- Decide whether two lists are statistically different or not.
- Each subject will have statistical result for each channel.
- Then, overall results are shown as percentage.

Above procedure generates two lists that show difference of artifact removal performance. It was desired that there must not be statistical difference for non-artifactual segments and must be statistical difference for artifactual parts. To examine results statistically, ttest was used. Ttest is used to compare two averages and says significance of difference of two populations. Basically, it checks whether this difference has occurred by chance or not.In this analysis, paired ttest was used.

3.5. Source Localization

Artifact removal step eliminated ocular artifacts. Then, those signals were given as input to the source localization algorithm to find source parameters on the cortex. Source activities that cause potential difference depends on location of electrode and source, orientation or strength of sources and conduction properties of medium. By regarding these information, there are two important steps for source localization. First one is grid search and the second one is dipole fitting but before these two processes, ICA was performed again to obtain independent components. More importantly, JADE algorithm was used in this step. Then, each component was used to find particular sources by using these two steps.

$$X_k = f(r, m, e_k) \tag{3.2}$$

Model for localization is shown above. k is number of electrode. e_k is location of kth electrode. r is location of dipole in 3-D, m is moment magnitude and X_k is scalp potential value. This formula can also be stated due to linear relation of m and x. o is orientation of dipole at location of r [53]. In addition, f is attenuation function of dipole according to spatial metrics such as recording positions of electrode, location of dipoles and head model.

$$X_k(t) = m(t)f(r, o, e_k) \tag{3.3}$$

First, head model was selected. "Boundary Element Model" was used that consists of three-shell structure that are skin, skull and cortex. It was obtained from MNI (Montreal Neurological Institute) canonical template brain. Secondly, grid search procedure was started. Although its results were not accurate, it provides convenient starting points for dipole fitting in the next step. Grid search basically covers whole brain and initially finds ideal source locations in 3-D by computing forward model (dipole to electrode projections) for every grid location. After that, comparison of grid location with topographies of whole components was done.

Grid search was done by looking at locations and orientations. Then, potential value of dipole source is calculated with the below formula. Moreover, S is source potential, C is conductor matrix, U is recorded potential at scalp. Residual variance (RV) of unmodeled part of signal is calculated by looking at difference of measured and modeled data. Then, source parameters (location and orientation) are iteratively changed. This process is called non-linear least squares. Parameter changing goes on until RV reaches an acceptable level. All in all, source parameter change algorithm tries to minimize the difference between the actual and model data.

$$S = C^{-1}U \tag{3.4}$$

In our data analysis, dipoles with residual variance lower than 15% were used in further analyses. Activations in Brodmann areas were ordered according to the number of localized dipoles. Areas with low number of dipoles were omitted from analyses (<10% of total dipoles). After higher residual variances were eliminated, Talairach coordinate transform operation was performed and Brodmann areas were found. In the following step, location and moment magnitude of the dipole was used to model. More importantly, dipole magnitudes were normalized through dividing each magnitude by the mean of subject's overall dipole magnitude . Moreover, source localization was performed in EEGLAB v14 installed in MATLAB software.

3.6. Talairach Coordinates Matching

Talairach Coordinate Matching helps researchers to assign Talairach Atlas labels for a given {x,y,z} coordinate. There is a hierarchy that has 5 levels. Those are hemisphere, lobe, gyrus, tissue type, and cell type. After {x,y,z} locations were given as input, information in terms of anatomy was generated. Results of this operation was shown in the corresponding part of the results section. This transform was performed using the software of the given references. [55, 56].

3.7. Multiple Regression

In the previous step, anatomical regions' interpretation of localized dipoles was done. In this step, those areas were modeled by using multiple regression in SPPS v25 software. To model results, performance change (net score, attempt number and correct answer number) was used as dependent variables and moment magnitude of Brodmann areas were used as independent variables.

3.8. Frontal Asymmetry and Power Spectrum

Frontal asymmetry can also be a biomarker of motivational change. In this study, frontal channels at F3-F4 and F7-F8 were used to model performance change. In addition, alpha band power of signals were used to find correlations with performance change. Obtained results were displayed in the next section. This calculation was performed in MATLAB software with custom code.

4. RESULTS

4.1. Behavioral Results

After performance feedback was given, score change was evaluated and it was observed that the feedback type (Positive-Negative) induced a performance change in terms of net score change, number of attempted questions and the number of correct answers.

Another evaluation was done on the effects of trial performance. There were 10 trials and it was desired that performance measures throughout the duration of the experiment for both positive and negative feedbacks were not affected. As seen in Figure 4.1 and 4.2 trial number did not change performance for PF-NF for feedback conditions visually. The same analysis was done for the number of attempted questions and the number of correct answers and then similar results were obtained. It was concluded that performance change did not show a trial-based trend.

Figure 4.1. Net Score Change After Negative Feedback

Table 4.1. Behavioral Results of Positive Feedback

Subject	**Net Score Change**	**Correct Answer Change**	**Attempt Number Change**
Subject 1	-1.70	-1.5	-0.66
Subject 2	-1.2	-1	0
Subject 3	-0.57	-0.57	-0.57
Subject 4	-0.75	-0.83	-1.16
Subject 5	-2.20	-2.16	-1.66
Subject 6	0	0	0
Subject 7	-0.25	-0.25	-1
Subject 8	-0.03	0	0.14
Subject 9	-0.91	-1	-0.66
Subject 10	-0.5	-0.6	-1
Subject 11	0.04	0.16	0.83
Subject 12	-0.93	-1	-1.25
Subject 13	-0.66	-0.66	-0.66
Subject 14	-1.15	-1.2	-1.4
Average	-0.77	-0.75	-0.64

Table 4.2. Behavioral Results of Negative Feedback

Subject	**Net Score Change**	**Correct Answer Change**	**Attempt Number Change**
Subject 1	2.6	2.5	1.75
Subject 2	1.25	1.2	1
Subject 3	1.16	1.33	2
Subject 4	1.43	1.5	1.5
Subject 5	-0.31	-0.5	-1.25
Subject 6	0.62	0.66	0.66
Subject 7	2.54	2.33	1.33
Subject 8	2.33	2	0.33
Subject 9	1.12	1	-0.25
Subject 10	1.4	1.4	1.2
Subject 11	-0.18	0	1
Subject 12	0.75	0.66	-0.5
Subject 13	1.17	1.14	1.14
Subject 14	3.15	3.2	3.4
Average	1.36	1.31	0.95

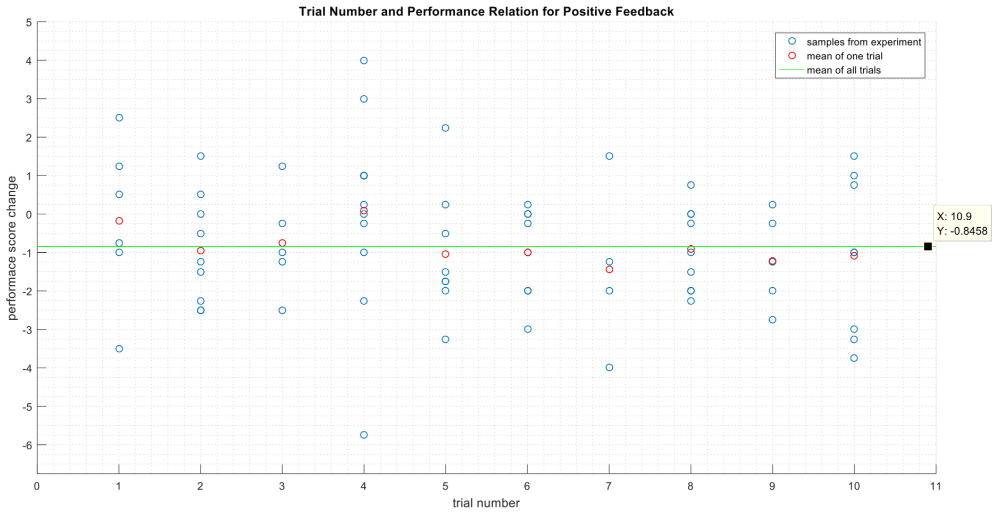

Figure 4.2. Net Score Change After Positive Feedback

4.2. EEG Analysis

4.2.1. Artifact Removal Results

An example of artifact removal results is shown in fig 4.3. The top trace is raw EEG signal before it was processed with artifact removal algorithm. The lower 3 traces are the results of different artifact removal algorithms. It can be clearly seen that Croft's Regression was the worst and ICA's performance was the best one. Although adaptive filter generally can clean ocular effect, I observed some rounds which still displayed similar artifacts. It is important to know that ICA uses correlation based, ICA2 is variance based selection of components.

Firstly, artifactual segments were evaluated. In this step, higher percentage was better to ensure artifact removal was properly performed. The difference between raw EEG and ICA removed data was statistically significant in 79.76% for entire data. The data cleaned by adaptive filter showed a difference only in 47.37% of the samples. Also, AF and ICA results were compared and 24.70% of whole data came statistically different. Lastly, EEG-ICA2 and EEG-Croft's Regression come 72.46% and 97.0% respectively.

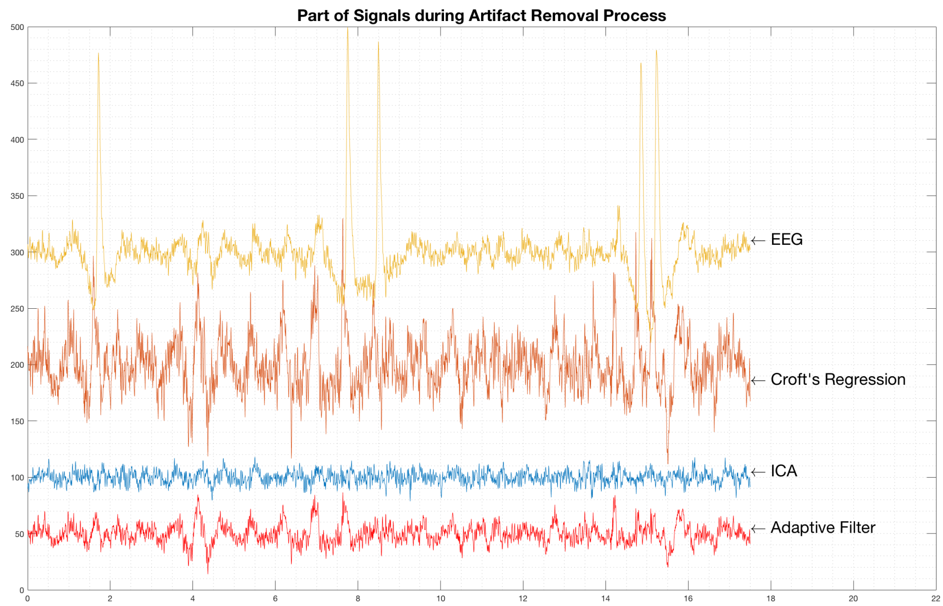

Figure 4.3. Artifact Removal Result

Secondly, non-artifactual segments were examined. In this step, lower percentage was better to prevent data loss. EEG-ICA displayed 36.03% which means that 36.03% non-artifactual segments in whole data changed statistically significantly. However, adaptive filter showed interesting result that was 49.80%. It caused data loss. Also, 28.34% of data was statistically significant for adaptive filter and ICA. Lastly, EEG-ICA2 and EEG-Croft's Regression come 49.79% and 89.30% respectively.

Thirdly, channel rms values were analyzed. EEG and ICA showed difference whose percentage was 88.66%. In addition, AF-EEG and ICA-AF distinction was came 55.87% and 24.13% respectively. Then, EEG-ICA2 and EEG- Croft's Regression come 74.49% and 93.13% respectively. As a result of this step, ICA shows good performance to get rid of artifacts but caused some data loss.

This procedure was then implemented for all subjects and trials-rounds. Finally, table was prepared to see big picture for artifact analysis. There were 3 different comparisons. These are artifactual, non-artifactual and channel rms performances. As stated previously, comparison was done between reference EEG (uncorrected data) and artifact removal method implemented methods which are ICA and AF. Table basically shows how much of total data was changed statistically significantly during artifact removal process.

Table 4.3. Percentage Table

Percentage of Significant Differences in the Compared Datasets			
Comparison	Artifactual RMS	Non-artifactual RMS	Channel RMS
EEG-ICA	79.76%	36.03%	88.66%
EEG-AF	47.37%	49.80%	55.87%
AF-ICA	24.70%	28.34%	27.13%
EEG-ICA2	72.46%	49.79%	74.49%
EEG-Regresyon	97.00%	89.30%	93.13%

Average rms values were also plotted to see channel by channel differences. In the figure 4.4, artifactual segments' rms values were compared. Frontal channels that have much more than eye-related artifacts showed the highest decrement. Fz, F7 and F8 also showed similar effect. Channels that were on the backside displayed lower change.

In the following figure 4.5, non-artifactual segments' rms comparison was done. As shown in figure, frontal channels were affected negatively and rms values decreased after artifact removal. Other channels that are far away from frontal part, did not show crucial decrement. All in all, artifact removal caused some data loss especially for frontal channels.

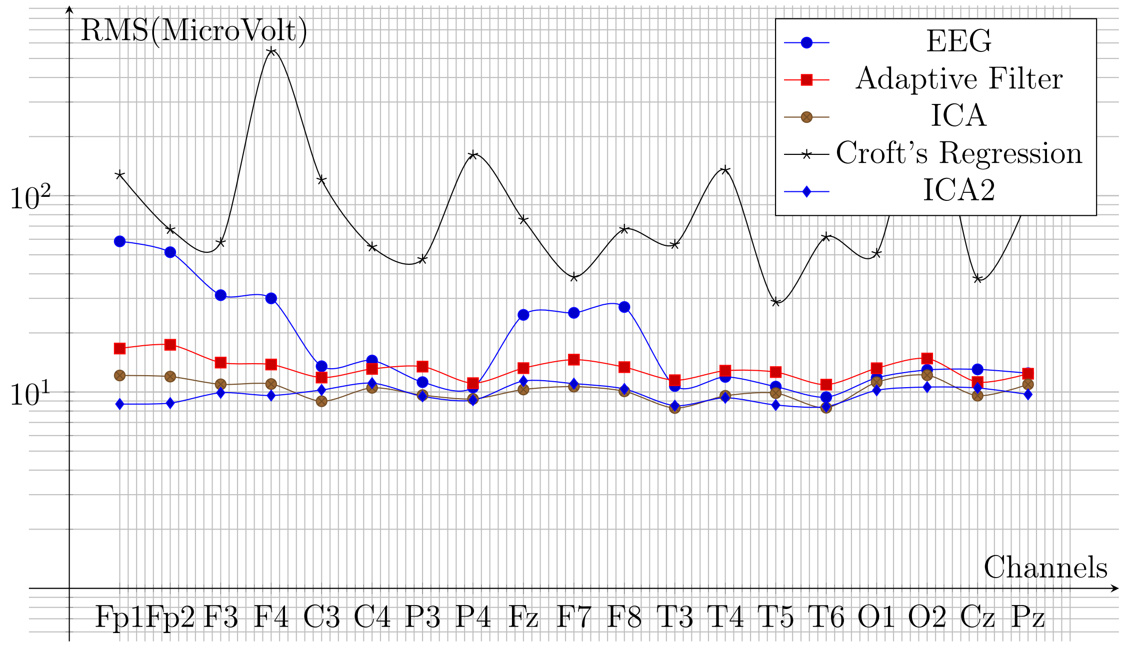

Figure 4.4. Artifactual Segments-RMS Comparison

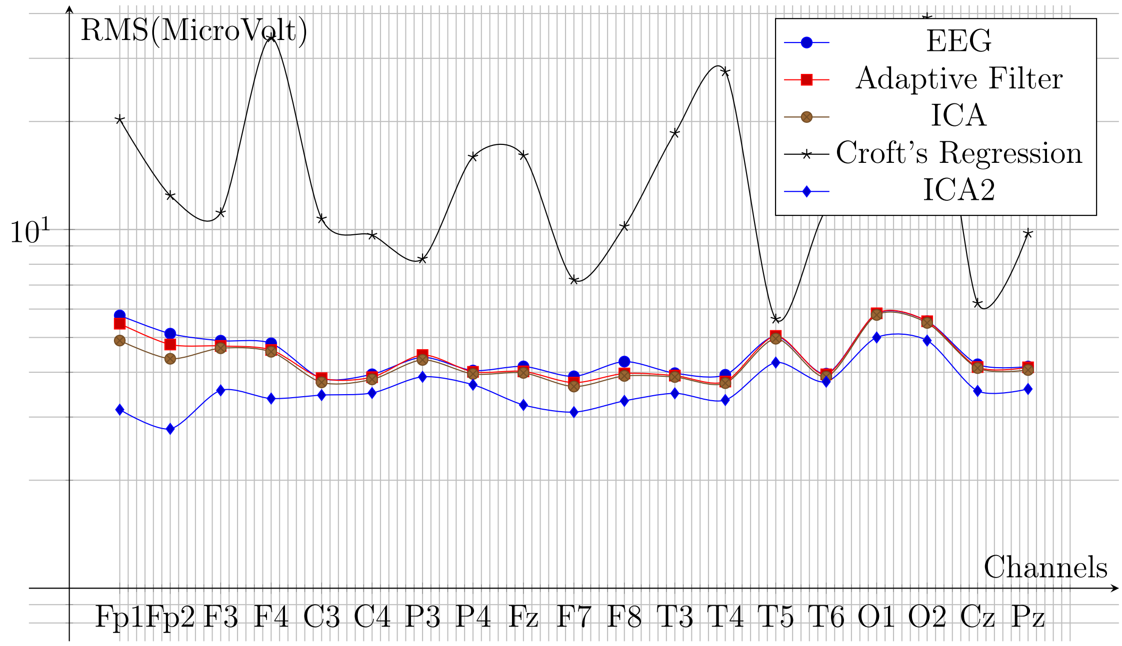

Figure 4.5. Non-Artifactual Segments-RMS Comparison

4.2.2. Source Localization Results

In this section, source localization results will be explained. Figure 4.6 displays result of source localization step visually. Dipoles had {x,y,z} coordinate information, corresponding component number and residual variance (% dipole not fitted) of component. Dipole location can be seen in 3D. In the following table 4.4 shows result of talairach coordinate transform. Source localization provides information until moment magnitude line. Talairach transform generates following lines that are Level 1-5 and Range. They are basically anatomical meaning of this location.

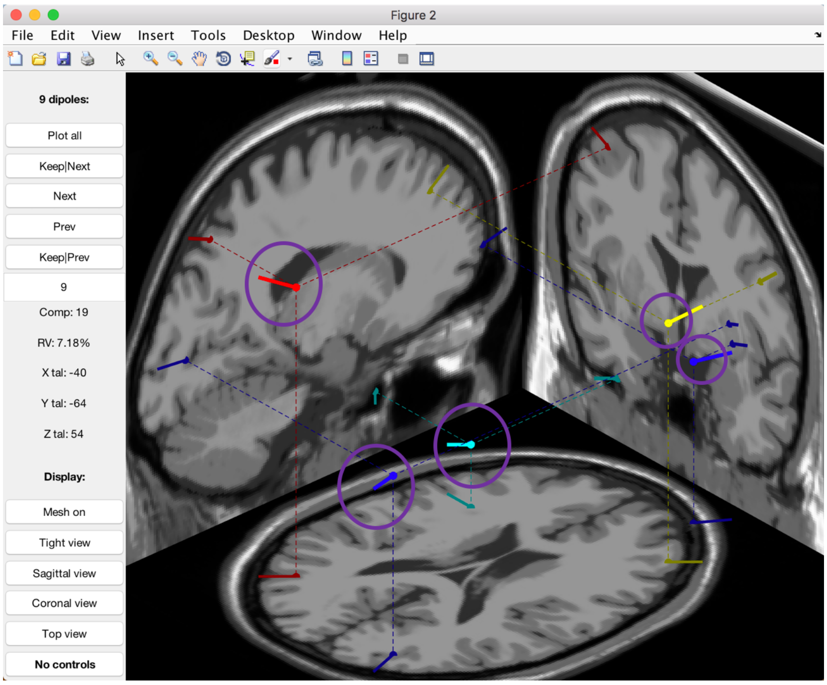

Figure 4.6. One of the Results of Dipole Fitting Process

Table 4.4. Talairach Coordinate Transform Result

Subject No	1
Trial	1
Round	1
Residual Variance	0,09082208702
X Coord. (mm)	-61,72138689
Y Coord. (mm)	-47,68199788
Z Coord. (mm)	44,38599594
Normalized Moment Magnitude	0,2069382393
Level 1	Left Cerebrum
Level 2	Parietal Lobe
Level 3	Inferior Parietal Lobule
Level 4	Gray Matter
Level 5	Brodmann area 40
Range (mm)	2

In addition, active dipole numbers were shown in tabular form in table (4.5,4.6 and 4.7) in Brodmann areas for 3 rounds(2 Round + 1 Feedback Interval). Whole rounds includes both positive and negative feedback caused dipoles to see big picture of dipole numbers.

Table 4.5. Round 1 Dipole Results

Round 1 Dipole Results

Regions	**Number of Dipoles**	%
Premotor cortex and Supplementary Motor cortex	101	19,1
Associative visual cortex	63	11,9
Dorsolateral prefrontal cortex	52	9,8
Anterior prefrontal cortex	44	8,3
Includes Frontal eye fields	41	7,7
Somatosensory Association Cortex	38	7,2
Supramarginal Gyrus	23	4,3
Middle Temporal gyrus	20	3,7
Orbitofrontal area	17	3,2
Dorsal posterior cingulate Cortex	15	2,8
Primary Somatosensory Cortex	14	2,6
Dorsal Anterior cingulate cortex	14	2,6
Secondary visual Cortex	13	2,4
Ventral Anterior cingulate Cortex	13	2,4
Inferior Temporal gyrus	10	1,8
Superior Temporal gyrus	9	1,7
Pars orbitalis	8	1,5
Primary Motor Cortex	8	1,5
Angular Gyrus	7	1,3
Primary gustatory cortex	6	1,1
Ventral posterior cingulate cortex	3	0,5
Primary visual Cortex	3	0,5
Fusiform Gyrus	2	0,3
Insular Cortex	2	0,3
Part of Anterior cingulate Cortex	1	0,1
Ventral entorhinal cortex	0	0

Table 4.6. Round 2 Dipole Results

Round 2 Dipole Results

Regions	**Number of Dipoles**	%
Premotor cortex and Supplementary Motor cortex	99	18,6
Associative visual cortex	57	10,7
Dorsolateral prefrontal cortex	52	9,7
Anterior prefrontal cortex	43	8,0
Somatosensory Association Cortex	42	7,9
Includes Frontal eye fields	33	6,2
Supramarginal Gyrus	29	5,4
Ventral Anterior cingulate Cortex	22	4,1
Dorsal posterior cingulate Cortex	21	3,9
Secondary visual Cortex	20	3,7
Orbitofrontal area	18	3,3
Superior Temporal gyrus	13	2,4
Primary Somatosensory Cortex	12	2,2
Dorsal Anterior cingulate cortex	12	2,2
Middle Temporal gyrus	11	2,0
Pars orbitalis	10	1,8
Primary Motor Cortex	8	1,5
Inferior Temporal gyrus	7	1,3
Angular Gyrus	6	1,1
Insular Cortex	5	0,9
Ventral posterior cingulate cortex	3	0,5
Primary gustatory cortex	2	0,3
Part of Anterior cingulate Cortex	2	0,3
Primary visual Cortex	2	0,3
Fusiform Gyrus	1	0,1
Ventral entorhinal cortex	1	0,1

Table 4.7. Feedback Round Dipole Results

Feedback Interval Dipole Results

Regions	**Number of Dipoles**	%
Premotor cortex and Supplementary Motor cortex	71	20,4
Associative visual cortex	43	12,3
Somatosensory Association Cortex	37	10,6
Anterior prefrontal cortex	29	8,3
Dorsolateral prefrontal cortex	28	8,0
Secondary visual Cortex	15	4,3
Supramarginal Gyrus	13	3,7
Dorsal posterior cingulate Cortex	13	3,7
Dorsal Anterior cingulate cortex	12	3,4
Includes Frontal eye fields	12	3,4
Angular Gyrus	10	2,8
Primary Somatosensory Cortex	9	2,5
Orbitofrontal area	8	2,2
Ventral Anterior cingulate Cortex	8	2,2
Inferior Temporal gyrus	8	2,2
Middle Temporal gyrus	7	2,0
Pars orbitalis	6	1,7
Primary Motor Cortex	5	1,4
Superior Temporal gyrus	3	0,8
Ventral posterior cingulate cortex	3	0,8
Primary gustatory cortex	2	0,5
Insular Cortex	2	0,5
Fusiform Gyrus	1	0,2
Part of Anterior cingulate Cortex	1	0,2
Primary visual Cortex	1	0,2
Ventral entorhinal cortex	1	0,2

4.2.3. Statistical Results

In this step, statistical results of modeled dipoles are shown. The following figures (4.7 and 4.8) show sample results for positive and negative feedback for randomly selected rounds.

Coefficients[a]

Model		Unstandardized Coefficients B	Unstandardized Coefficients Std. Error	Standardized Coefficients Beta	t	Sig.
1	(Constant)	-.215	.214		-1.007	.315
	Secondary_Visual_Cortex	.422	.682	.045	.618	.537
	Associative_Visual_Cortex	-1.486	.580	-.197	-2.562	.011
	Angular_Gyrus	-.348	.694	-.037	-.501	.617
	Premotor_Cortex	-1.223	.546	-.180	-2.240	.026
	Dorsolateral_Prefrontal_Cortex	-1.468	1.225	-.089	-1.199	.232
	Supramarginal_Gyrus	-3.024	2.863	-.077	-1.056	.292
	Somatosensory_Ass_Cortex	-1.201	.760	-.120	-1.579	.116
	Primary_Somatosensory_Cortex	.349	1.048	.024	.333	.740
	Dorsal_Anterior_Cingulate_Cortex	-.311	1.571	-.015	-.198	.843
	Includes_Frontal_Eye_Fields	-.582	1.118	-.038	-.521	.603
	Anterior_Prefrontal_Cortex	.344	.371	.070	.927	.355
	Orbitofrontal_Area	-1.063	.456	-.170	-2.332	.021
	Dorsal_Posterior_Cingulate_Cortex	-1.184	1.353	-.065	-.875	.383
	Ventral_Anterior_Cingulate_Cortex	-4.513	2.101	-.157	-2.148	.033
	Primary_Motor_Cortex	-3.959	2.097	-.139	-1.888	.061
	Middle_Temporal_Gyrus	-.008	.125	-.005	-.065	.948
	Inferior_Temporal_Gyrus	.017	.089	.014	.191	.849

a. Dependent Variable: Net_Score

Figure 4.7. Positive Feedback Results at Feedback Interval with Net Score Change

The analysis was done for both attempt number and correct answer changes. Below tables (4.8 and 4.9) shows positive feedback and negative feedback results, respectively. Moreover, only significant results were shown as (+) or (-) signs. (+) sign means that activation in this area caused positive performance change. On the other hand, (-) sign means that activation in this region caused negative performance change. In the second row, Net Score, Correct Answer and Attempted Number means dependent variables in the used model.

Coefficients[a]

Model		Unstandardized Coefficients B	Unstandardized Coefficients Std. Error	Standardized Coefficients Beta	t	Sig.
1	(Constant)	1.054	.295		3.569	.000
	Secondary_Visual_Cortex	-.371	.559	-.048	-.663	.508
	Associative_Visual_Cortex	-1.312	.740	-.132	-1.773	.078
	Premotor_Cortex	.567	.645	.066	.878	.381
	Dorsolateral_Prefrontal_Cortex	1.830	.883	.154	2.072	.040
	Supramarginal_Gyrus	1.733	2.116	.059	.819	.414
	Somatosensory_Ass_Cortex	2.058	1.209	.127	1.702	.090
	Primary_Somatosensory_Cortex	-.567	4.850	-.008	-.117	.907
	Dorsal_Anterior_Cingulate_Cortex	2.612	1.371	.138	1.905	.058
	Includes_Frontal_Eye_Fields	2.061	3.039	.049	.678	.498
	Anterior_Prefrontal_Cortex	.441	.538	.060	.820	.413
	Orbitofrontal_Area	.506	.452	.080	1.119	.265
	Dorsal_Posterior_Cingulate_Cortex	-2.478	2.437	-.073	-1.017	.311
	Ventral_Anterior_Cingulate_Cortex	.504	2.538	.014	.199	.843

a. Dependent Variable: Net_Score

Figure 4.8. Negative Feedback Results at Feedback Round

According to positive feedback results significant correlations were found between net score and some Brodmann areas in feedback interval. These were Premotor and Supplementary Motor Cortex, Orbitofrontal Area, Ventral Anterior Cingulate Cortex and Associative Visual Cortex. In addition, correct answer was another performance change metric and similar significant results with net score were found in feedback interval. The last metric was number of attempted questions. Interestingly, Round 1 and feedback interval showed different activation patterns when compared with other metrics. In Round 1, Somatosensory Association Cortex and Dorsal Anterior Cingulate Cortex display significant activations. In addition, Secondary Visual Cortex showed activation in feedback interval.

According to negative feedback results, Secondary Visual Cortex become significant in the first round when net score and correct answer were used. In the Round 2, Middle Temporal Gyrus become active for all three metrics (net score, correct answer and attempt number). Moreover, Dorsal Anterior Cingulate cortex was another active

Table 4.8. Positive Feedback Results

	Net Score			**Correct Answer**			**Attempted Number**		
Brodmann Areas	R1	R2	R3	R1	R2	R3	R1	R2	R3
Secondary Visual Cortex									+
Superior Temporal Gyrus									
Associative Visual Cortex			-			-			
Angular Gyrus									
Premotor and Suppl. Motor Cortex			-			-			
Dorsolateral Prefrontal Cortex									
Supramarginal Gyrus									
Somatosensory Association Cortex							-		
Primary Somatosensory Cortex									
Dorsal Anterior Cingulate Cortex							+		
Primary Gustatory Cortex									
Includes Frontal Eye Fields									
Anterior Prefrontal Cortex									
Pars Orbitalis									
Orbitofrontal Area			-			-			
Fusiform Gyrus									
Dorsal Posterior Cingulate Cortex									
Ventral Anterior Cingulate Cortex			-			-			
Primary Motor Cortex									
Middle Temporal Gyrus									
Inferior Temporal Gyrus									
Ventral Posterior Cingulate Cortex									
Insular Cortex									
Part of Anterior Cingulate Cortex									
Primary Visual Cortex									
Ventral Entorhinal Cortex									

area according to number of attempted questions in round 2. When the feedback round (R3) was evaluated, Dorsal Anterior Cingulate Cortex become active for all three metrics. Also, there were another significant results in Dorsolateral Prefrontal Cortex when net score and correct answer were used as performance change in feedback round.

Table 4.9. Negative Feedback Results

	Net Score			Correct Answer			Attempted Number		
Brodmann Areas	R1	R2	R3	R1	R2	R3	R1	R2	R3
Secondary Visual Cortex	-			-					
Superior Temporal Gyrus									
Associative Visual Cortex									
Angular Gyrus									
Premotor and Suppl. Motor Cortex									
Dorsolateral Prefrontal Cortex			+			+			
Supramarginal Gyrus									
Somatosensory Association Cortex									
Primary Somatosensory Cortex									
Dorsal Anterior Cingulate Cortex			+			+		+	+
Primary Gustatory Cortex									
Includes Frontal Eye Fields									
Anterior Prefrontal Cortex									
Pars Orbitalis									
Orbitofrontal Area									
Fusiform Gyrus									
Dorsal Posterior Cingulate Cortex									
Ventral Anterior Cingulate Cortex								+	
Primary Motor Cortex									
Middle Temporal Gyrus		+			+			+	
Inferior Temporal Gyrus									
Ventral Posterior Cingulate Cortex									
Insular Cortex									
Part of Anterior Cingulate Cortex									
Primary Visual Cortex									
Ventral Entorhinal Cortex									

In addition to previous analysis, another hypothesis to be answered is gender based differences. Table 4.10 and 4.11 show active regions in the positive feedback round for female and male subjects. Only statistically significant areas were shown instead of whole results. According to female results, only sensory areas were active but male results were much more meaningful in terms of motivational concepts when positive feedback was given. On the other hand, negative feedback caused motivational areas for both male and female.

Table 4.10. Female Positive Feedback Results

Brodmann Areas	Net Score	Correct Answer	Attempt Number
Associative Visual Cortex	-1.13(0.020)	-1.30(0.013)	
Secondary Visual Cortex			1.57(0.030)
Primary Somatosensory Cortex			4.44(0.011)

Table 4.11. Male Positive Feedback Results

Brodmann Areas	Net Score	Correct Answer	Attempt Number
Premotor Cortex	-1.74(0.035)	-1.53(0.057)	
Anterior Prefrontal Cortex			1.70(0.036)
Inferior Temporal Gyrus			1-2.66(0.055)

Moreover, negative feedback related activations based on gender differences were investigated. Only significant results were shown in the following tables.

Table 4.12. Female Negative Feedback Results

Brodmann Areas	Net Score	Correct Answer	Attempt Number
Somatosensory Association Cortex	2.77(0.045)		
Dorsalateral Prefrontal Cortex	2.55(0.053)	2.14(0.053)	

Table 4.13. Male Negative Feedback Results

Brodmann Areas	Net Score	Correct Answer	Attempt Number
Dorsal Anterior Cingulate Cortex	3.49(0.030)	3.48(0.028)	3.5(0.032)

Another interesting analysis was to seek differences in feedback interval for positive-negative feedbacks. Firstly, areas that had lower number of dipoles and non-coincident areas were eliminated. Then, remaining area dipoles were compared to measure statistical significance. As a result of this study, there was no active significant areas. Moreover, this comparison was done for Round 2 and Round 1 regarding positive and negative feedbacks. Although positive feedback did not cause significance activations, negative feedback caused significant activation in Primary Motor Cortex (p value = 0.03) when Round 2 and Round 1 were compared.

4.2.4. Frontal Asymmetry Results

Frontal asymmetry calculation was done for F3/F4 and F7/F8 channels based on alpha band (8-12 Hz). The first analysis was to seek differences in FA value in response to positive or negative feedback. To do that, ttest was used to understand data from PF and NF come from activations with unequal mean. As a result of this analysis, both F3/F4 (h=0, p=0.88) and F7/F8 (h=0, p=0.61) results cannot reject null hypothesis. It was concluded that PF-NF generated similar statistical results based on Frontal Asymmetry.

In addition, more activation at left than right may express something related to motivation. From this perspective, results were evaluated again by comparing activations in F3/F4 channels. According to results, more left than right activations account for 51.06% of Negative Feedback Round and 47.05% of Positive Feedback Round.

4.2.5. Power Spectrum Results

Another analysis was done to find significant changes between Round2 and Round1 respectively. This analysis includes power changes alpha band (8-12 Hz). Round2 and Round1 difference in 19 channels were used as independent variables to predict performance change. Also, F3/F4 and F7/F8 ratios were used as independent variables. Results of this analysis were shown in the following tables 4.14 and 4.15. First number is coefficient of particular channel on performance change and second number in parenthesis shows significance level respectively.

Table 4.14. Alpha Band Power Change Results for Negative Feedback

Channels	Net Score	Correct Answer	Attempt Number
F4	-0.35(0.03)	-0.33(0.02)	
C3	-1.42(0.03)	-1.37(0.02)	-1.36(0.01)
P4			-0.84(0.03)

Table 4.15. Alpha Band Power Change Results for Positive Feedback

Channels	Net Score	Correct Answer	Attempt Number
Fp2			-0.67(0.04)
F4	0.80(0.02)	0.74 (0.02)	
O1		0.21(0.04)	0.33(0.01)
O2	-0.20(0.05)	-0.22(0.02)	-0.34(0.01)

As a result of this study, it was concluded that frontal channels generated some significant results regarding literature results. F4 channel alpha band power change affected performance in both type of feedbacks. More interestingly, after positive feedback was given, Fp2 power activation in this band also affected attempt number negatively. Moreover, C3, O1 and O2 channels also generated crucial results. Although there was no enough evidence for those channels except F4 and Fp2 in the literature, it is being studied as future work.

5. DISCUSSION

5.1. General conclusions

Results section includes active brain regions and significant channels related to performance changes. After that, one the of the most important steps is to interpret these activations and results in terms of functionality of these areas and common points with literature studies.

According to feedback interval, results of net score and the number of correct answers are significantly correlated with Associative Visual Cortex, Premotor and Supplementary Motor Cortex, Ventral Anterior Cingulate Cortex and Orbitofrontal areas when positive feedback is given.

Associative Visual cortex functions includes spatial working memory, visual pattern detection, feature-based attention, visual memory recognition etc. and those activations may be due to questions of experiments instead of reward-related activations but interestingly this area was also found in a similar study. Subjects that were given positive feedback activate this area much more when compared with negative feedback. This situation was attributed to planning of movements [65]. Moreover, Feedback Interval-Attempted number in PF model, Secondary Visual Cortex become active significantly. This field is the second greatest area in visual cortex. One of its functions is to transfer received connection to other part in the visual cortex. Also, recently announced that this field take a role to save object recognition memory for transfer it from short-term to long-term memories [66]. Another area was Premotor and Supplementary Motor Cortex which is responsible sensory guidance of movement, muscles control, word retrieval, planning, solving of novel problems and basically motor functions etc. [67]. According to activations in those three regions, it was concluded that these were not so relevant with neuroeconomics field.

Ventral part of Anterior Cingulate Cortex is connected to amygdala, nucleus accumbens hippocampus and hypothalamus. While ACC generally deals with reward anticipation, decision-making, control of impulse and emotion, ventral part of this region evaluates emotional and motivational information [68]. In addition, ACC had strong connections with motor systems [69]. vACC is much more interesting than other fields due to the fact that it may be responsible for performance change due emotional effect. Some studies in monkeys found this region connected with limbic regions such as hypothalamus, amygdala, hippocampus and striatum that were responsible from emotional and reward processing [70–73]. This area becomes active during feedback interval and there was negative relation between performance change and this area's activation.

Orbitofrontal area was another active region in feedback interval for modeling with net score and correct answer change. This area is on the ventral surface of the frontal lobe of the brain. It also connected reward processing regions similar with ACC. It mainly deals with cognitive processing of decision making and represents emotion and reward in this decision making process. Although OFC and ACC share some common points, they have distinguished properties. Firstly, OFC and ACC had strong connection to reward-related areas but their different connections provide distinct computational processes during decision making. OFC encodes value of an object but plays lesser role for determining cost of action due to lower connections with motor areas. All in all, reward related decision making role of this region is meaningful in terms of neuroeconomics [8].

Another interesting result comes from attempted number instead of net score and correct answer change. In the first round, Dorsal Anterior Cingulate Cortex and Somatosensory Association Cortex were active regions to be interpreted. SAc receives sensory information from the body and these are feelings of skin, visual, pain or auditory stimuli information respectively. This function is not relevant in terms of neuroconomics hypothesis but dACC played much more interesting role in this model. More activations in this region in Round 1 caused more willingly to attempt questions. When it was interpreted in terms of functionality, it was suggested that this field plays role in reward-based decision making especially this field guides behavior by including motivation, detecting goals, encoding reward values... embedding information with help of other connected cells in the internal network and then influences motor preparation and responses [33].

After positive feedback results were evaluated, the next issue is to examine negative feedback results with neuroconomics perspective. In the first rounds of NF, Secondary Visual Cortex becomes active in the model that has net score and correct answer change as dependent variable. This field especially shares common functions with primary visual cortex and cells inside of this structure deal with simple properties such as color, spatial frequency and orientation.

Furthermore, Round 2 results come out significant activations in Middle Temporal Gyrus and this result was common for all dependent variables (net score, correct answer, attempt number). When we look at the functionality of this region, this field may be related to increased motivation. This relationship was found very strong in Depasque's study [74]. They concluded motivational change is associated with activations in left medial temporal lobe. Similar relation was also stated in another study [75]. This finding may be interpreted as meaningful from neuroconomics experiment because this area was active for all performance models and coefficients were positive. Therefore, activations in this field may increase motivation and directly affects performance in positive way. Besides, attempted number model generated one more area in Round 2. This is Ventral Anterior Dorsal Anterior Cingulate Cortex and this region's importance was explained in previous paragraphs. In addition, dACC activations in feedback rounds for three metrics were crucial. It was stated that this region took a role in reward-based decision making, learning and performance of tasks and then functions of this area were influenced by dopamine [33]. According to results, this region can help to direct behaviors by integrating outside information to evaluate motivation and rewards, finding targets and finally allocate motor preparation and motor responses. This functionality can be seen crucial for interpreting of this issue.

According to feedback interval results, Dorsalateral Prefrontal Cortex becomes one of significant areas when net score and correct answer were modeled. In literature, this area was found to initiate motivated behavior but they attributed this to reward anticipation [32]. Moreover, authors stated that the reward information enters dopamin system at this dlPFC region and transmits particular areas. Furthermore, dlPFC was also found in studies related to social preferences. It was stated that this field becomes active when someone needs to apply self-control to overcome interest in order to prevent being punished [76]. In literature results part, it would be stated that this area was found active when rejecting unfair offers. Number of attempted questions in feedback interval model resulted also significant activation in dACC. This region was also found in Round 2 and explained. All in all, in our experiment, NF motivated subjects to change and adapt their behaviors positively. Dorsal Anterior Cingulate Cortex and Middle Temporal Gyrus activations played significant role when modeled with three performance metrics.

5.2. Comparison with the literature results

There are a lot of studies that deal with reward processing of brain in the literature. More specifically, feedback related reward is closer to this conducted study. After searching experimental results that have similar content with thesis, below studies were found.

First one is related to positive/negative performance feedback's neural effects in younger-older adults. The experiment related to finding arrows' direction shown on the screen in limited time. It was hypothesized that feedback would serve as reward and causes striatal activation and performance feedback will lead different effects on younger-older adults due to aging effect. Brain activations were investigated by fMRI. As a result this study, positive feedback elicited stronger activation in the striatum when comparing with negative feedback. In addition, putamen, left-amygdala, lingual gyrus, right-left superial frontal gyrus in the thalamus come more active for positive feedback. Also, stronger activation becomes in the visual cortex after positive feedback and the reason was stated as associated with planning of movements. More interestingly, no difference was found between younger-older adults for processing performance feedback. [65]

Secondly, different types of negative feedback such as confirmative and informative types were given subjects in another experiment that includes spatial-perception test. Subjects were selected one of the three figures by looking 3 criteria. fMRI was used to investigate brain dynamics. The items to be selected in the experiment were the largest size and cut-off angle, faster than average response time. After each trial, they were shown feedback like "You Failed" or "You Failed ! Size is not the biggest". According to results, confirmatory feedback causes emotional reactions in amygdala and dorsal anterior cingulate cortex. On the other hand, informative feedback caused activations in the dorsalateral prefrontal cortex. This area can be explained as cognitive control of negative emotions during failure experience. [77]

Thirdly, another time estimation (1second) experiment was conducted to see feedback effects on brain. In this scenario, there were 3 feedback types; those are positive-negative and No Feedback(uninformative). According to behavioral results, it was concluded that informative feedback increased performance when compared with uninformative feedback. In addition, fMRI and EEG were used to seek neural correlates of feedback on the brain. Although negative feedback did not cause statistical difference when compared with positive feedback, PF leads more activations on Rostral Anterior Cingulate Cortex, Right Superior Frontal Gyrus, Posterior Cingulate Cortex and Striatum (caudate/putamen). More significantly, there was a study in the literature which concluded that Posterior Cingulate Cortex is connected areas that is related to reward and orbitofrontal cortex and caudate nucleus are active due to expectation and delivery of reward [78, 79].

The next study was two choice gambling game. The subjects selected one of the options between 5 and 25 or 25 and 5 on the screen. They were then gain or loss this amount in random way. EEG-fMRI was employed at the same time to seek brain activations. Researchers also inspected theta (Negative Feedback) and high-beta (Positive Feedback) changes in power spectrum. In addition, fMRI results were evaluated. As a result, gain>loss situations caused activations in the ventral striatum, putamen, bilateral-lateral temporal gyrus and medial posterior areas. On the other hand, loss>gain results lead crucial activations with theta power in dACC and right Dorsalateral Prefrontal Cortex. Moreover, both feedbacks elicited power increment in examined power band but there was no significance between them [80].

Another study investigated brain responses to performance by recording from human cerebral cortex in epileptic patients. In the experiment, subjects estimated 1 second time by pressing button twice. After their performance, they were given PF-NF and no feedback for control group. When the results were evaluated, positive feedback caused activations in medial OFC, and dACC. However, negative feedback caused neural connections in the pre-supplementary Motor Area, DLPFC and lateral OFC [81].

Finally, when dACC related studies were evaluated in terms of functionality, dorsal anterior cingulate cortex (dACC) activation was not only considered for error detection. Authors state that this area monitors results of our actions to adapt behaviorally and it may provide a way for humans to correct or improve actions that have been done previously [81, 82]. Besides, this region was found generator of Feedback Related Negativity as a result of EEG source localization analysis in some studies [83–85]. This region was common for all models in Negative Feedback Interval (R3) in our conducted study.

5.3. Limitations of the study

First, signal processing algorithms that were used can be improved. For example: ICA displayed better performance according to other suggested methods but caused some data loss. To overcome this issue, canonical correlation analysis, wavelet based methods, combination of ICA, EMD, CCA may improve this step with less data loss for non-artifactual parts of signals. Furthermore, lack of performance metric for real time recorded EEG signals is a problem. Much more reliable methods that show performance change in artifact removal can provide better analyze for different AR algorithms.

In addition, source localization was done under some assumptions such as defining a standard head model. At this point, not all subjects had the same head structure and this may cause some localization error. Furthermore, EEG dipole results do not always come in the brain or gray matter. All dipoles in white matter were eliminated. Also, inverse problem does not have unique solution and this may complicate this process. Although EEG is not the best method for spatial localization, its lower cost and provision of consistent results like fMRI makes it still valuable. Especially, its high temporal resolutions allow researchers formulate interesting hypothesis for brain dynamics. Perhaps, more reliable source localization algorithms will make EEG much more preferred in the future.

Moreover, subjects were given positive or negative feedbacks. In literature, there were some studies with no feedback to be used it as baseline. Then, PF-NF comparison was done regarding contrast between PF-No FB and NF-No FB. This aspect may provide control group's behavior.

Finally, common head model for all subjects may cause wrong dipole results. To overcome this issue, static MR may be taken for each subject and everyone's head model can be used to find dipoles. However, this operation may be very costly. Furthermore, EEG device had 19 channels in the conducted study. EEG device with more channels can be used to reduce source localization error rate.

5.4. Future Work

Source localization is the one modeling options in the literature. There are different issues such as functional connectivity analysis to understand active regions' casual relationship. This is the next plan in this work. In addition, new methods for artifact removal increases very fast in the literature. If a method that is better than ICA can be found , it will be utilized in the future. Literature suggests wavelet based methods can also result good performance for artifact removal and implementation of some novel methods that over-performs ICA will be beneficial for the following analysis steps.

REFERENCES

1. De Martino, B., D. Kumaran, B. Seymour and R. J. Dolan, "Frames, biases, and rational decision-making in the human brain", *Science*, Vol. 313, No. 5787, pp. 684–687, 2006.

2. Tom, S. M., C. R. Fox, C. Trepel and R. A. Poldrack, "The neural basis of loss aversion in decision-making under risk", *Science*, Vol. 315, No. 5811, pp. 515–518, 2007.

3. McClure, S. M., D. I. Laibson, G. Loewenstein and J. D. Cohen, "Separate neural systems value immediate and delayed monetary rewards", *Science*, Vol. 306, No. 5695, pp. 503–507, 2004.

4. Yeung, N. and A. G. Sanfey, "Independent coding of reward magnitude and valence in the human brain", *Journal of Neuroscience*, Vol. 24, No. 28, pp. 6258–6264, 2004.

5. He, P., G. Wilson and C. Russell, "Removal of ocular artifacts from electro-encephalogram by adaptive filtering", *Medical and biological engineering and computing*, Vol. 42, No. 3, pp. 407–412, 2004.

6. Gneezy, U., M. Niederle and A. Rustichini, "Performance in competitive environments: Gender differences", *The Quarterly Journal of Economics*, Vol. 118, No. 3, pp. 1049–1074, 2003.

7. Camerer, C. F., "Goals, methods, and progress in neuroeconomics", *Annu. Rev. Econ.*, Vol. 5, No. 1, pp. 425–455, 2013.

8. Glimcher, P. W. and A. Rustichini, "Neuroeconomics: the consilience of brain and decision", *Science*, Vol. 306, No. 5695, pp. 447–452, 2004.

9. Bernheim, B. D., "On the potential of neuroeconomics: A critical (but hopeful)

appraisal", *American Economic Journal: Microeconomics*, Vol. 1, No. 2, pp. 1–41, 2009.

10. Fehr, E. and A. Rangel, "Neuroeconomic Foundations of Economic Choice–Recent Advances", *Journal of Economic Perspectives*, Vol. 25, No. 4, pp. 3–30, 2011.

11. Camerer, C., G. Loewenstein and D. Prelec, "Neuroeconomics: How neuroscience can inform economics", *Journal of economic Literature*, Vol. 43, No. 1, pp. 9–64, 2005.

12. Sanfey, A. G., J. K. Rilling, J. A. Aronson, L. E. Nystrom and J. D. Cohen, "The neural basis of economic decision-making in the ultimatum game", *Science*, Vol. 300, No. 5626, pp. 1755–1758, 2003.

13. Güçlü, B., S. Ertaç, A. Hortaçsu and J. A. List, "Mental attributes and temporal brain dynamics during bargaining: EEG source localization and neuroinformatic mapping", *Social neuroscience*, Vol. 7, No. 2, pp. 159–177, 2012.

14. Platt, M. L. and S. A. Huettel, "Risky business: the neuroeconomics of decision making under uncertainty", *Nature neuroscience*, Vol. 11, No. 4, p. 398, 2008.

15. Botvinick, M. M., T. S. Braver, D. M. Barch, C. S. Carter and J. D. Cohen, "Conflict monitoring and cognitive control.", *Psychological review*, Vol. 108, No. 3, p. 624, 2001.

16. Miller, E. K. and J. D. Cohen, "An integrative theory of prefrontal cortex function", *Annual review of neuroscience*, Vol. 24, No. 1, pp. 167–202, 2001.

17. Tversky, A. and D. Kahneman, "Advances in prospect theory: Cumulative representation of uncertainty", *Journal of Risk and uncertainty*, Vol. 5, No. 4, pp. 297–323, 1992.

18. Tversky, A. and D. Kahneman, "The framing of decisions and the psychology of

choice", *Science*, Vol. 211, No. 4481, pp. 453–458, 1981.

19. Novemsky, N. and D. Kahneman, "The boundaries of loss aversion", *Journal of Marketing research*, Vol. 42, No. 2, pp. 119–128, 2005.

20. Knutson, B., G. W. Fong, C. M. Adams, J. L. Varner and D. Hommer, "Dissociation of reward anticipation and outcome with event-related fMRI", *Neuroreport*, Vol. 12, No. 17, pp. 3683–3687, 2001.

21. Breiter, H. C., I. Aharon, D. Kahneman, A. Dale and P. Shizgal, "Functional imaging of neural responses to expectancy and experience of monetary gains and losses", *Neuron*, Vol. 30, No. 2, pp. 619–639, 2001.

22. Delgado, M., H. Locke, V. A. Stenger and J. Fiez, "Dorsal striatum responses to reward and punishment: effects of valence and magnitude manipulations", *Cognitive, Affective, & Behavioral Neuroscience*, Vol. 3, No. 1, pp. 27–38, 2003.

23. Knutson, B., C. M. Adams, G. W. Fong and D. Hommer, "Anticipation of increasing monetary reward selectively recruits nucleus accumbens", *Journal of Neuroscience*, Vol. 21, No. 16, pp. RC159–RC159, 2001.

24. Camerer, C., "Three cheers—psychological, theoretical, empirical—for loss aversion", *Journal of Marketing Research*, Vol. 42, No. 2, pp. 129–133, 2005.

25. Kahn, I., Y. Yeshurun, P. Rotshtein, I. Fried, D. Ben-Bashat and T. Hendler, "The role of the amygdala in signaling prospective outcome of choice", *Neuron*, Vol. 33, No. 6, pp. 983–994, 2002.

26. Kuhnen, C. M. and B. Knutson, "The neural basis of financial risk taking", *Neuron*, Vol. 47, No. 5, pp. 763–770, 2005.

27. Phelps, E. and R. Pollack, "Myopia and inconsistency in dynamic utility maximization", *The Review of Economic Studies*, Vol. 23, pp. 165–180, 1968.

28. Smith, E. E. and J. Jonides, "Storage and executive processes in the frontal lobes", *Science*, Vol. 283, No. 5408, pp. 1657–1661, 1999.

29. Sutton, S., P. Tueting, M. Hammer and G. Hakerem, "Evoked potentials and feedback", *Multidisciplinary perspectives in event-related potential research*, pp. 184–188, 1978.

30. Johnston, V. S., "Stimuli with biological significance", *Evoked brain potentials and behavior*, pp. 1–12, Springer, 1979.

31. Holroyd, C. B. and M. G. Coles, "The neural basis of human error processing: reinforcement learning, dopamine, and the error-related negativity.", *Psychological review*, Vol. 109, No. 4, p. 679, 2002.

32. Ballard, I. C., V. P. Murty, R. M. Carter, J. J. MacInnes, S. A. Huettel and R. A. Adcock, "Dorsolateral prefrontal cortex drives mesolimbic dopaminergic regions to initiate motivated behavior", *Journal of Neuroscience*, Vol. 31, No. 28, pp. 10340–10346, 2011.

33. Bush, G., B. A. Vogt, J. Holmes, A. M. Dale, D. Greve, M. A. Jenike and B. R. Rosen, "Dorsal anterior cingulate cortex: a role in reward-based decision making", *Proceedings of the National Academy of Sciences*, Vol. 99, No. 1, pp. 523–528, 2002.

34. Gehring, W. J. and R. T. Knight, "Prefrontal–cingulate interactions in action monitoring", *Nature neuroscience*, Vol. 3, No. 5, p. 516, 2000.

35. Luu, P., T. Flaisch and D. M. Tucker, "Medial frontal cortex in action monitoring", *Journal of Neuroscience*, Vol. 20, No. 1, pp. 464–469, 2000.

36. Carter, C. S., T. S. Braver, D. M. Barch, M. M. Botvinick, D. Noll and J. D. Cohen, "Anterior cingulate cortex, error detection, and the online monitoring of performance", *Science*, Vol. 280, No. 5364, pp. 747–749, 1998.

37. Barbati, G., C. Porcaro, F. Zappasodi, P. M. Rossini and F. Tecchio, "Optimization of an independent component analysis approach for artifact identification and removal in magnetoencephalographic signals", *Clinical Neurophysiology*, Vol. 115, No. 5, pp. 1220–1232, 2004.

38. Makeig, S., A. J. Bell, T.-P. Jung and T. J. Sejnowski, "Independent component analysis of electroencephalographic data", *Advances in neural information processing systems*, pp. 145–151, 1996.

39. Jung, T.-P., C. Humphries, T.-W. Lee, S. Makeig, M. J. McKeown, V. Iragui and T. J. Sejnowski, "Extended ICA removes artifacts from electroencephalographic recordings", *Advances in neural information processing systems*, pp. 894–900, 1998.

40. Jung, T.-P., C. Humphries, T.-W. Lee, S. Makeig, M. J. McKeown, V. Iragui and T. J. Sejnowski, "Removing electroencephalographic artifacts: comparison between ICA and PCA", *Neural Networks for Signal Processing VIII, 1998. Proceedings of the 1998 IEEE Signal Processing Society Workshop*, pp. 63–72, IEEE, 1998.

41. Sweeney, K. T., H. Ayaz, T. E. Ward, M. Izzetoglu, S. F. McLoone and B. Onaral, "A methodology for validating artifact removal techniques for physiological signals", *IEEE transactions on information technology in biomedicine*, Vol. 16, No. 5, pp. 918–926, 2012.

42. Joyce, C. A., I. F. Gorodnitsky and M. Kutas, "Automatic removal of eye movement and blink artifacts from EEG data using blind component separation", *Psychophysiology*, Vol. 41, No. 2, pp. 313–325, 2004.

43. Sweeney, K. T., S. F. McLoone and T. E. Ward, "The use of ensemble empirical mode decomposition with canonical correlation analysis as a novel artifact removal technique", *IEEE transactions on biomedical engineering*, Vol. 60, No. 1, pp. 97–105, 2013.

44. Croft, R. J. and R. J. Barry, "Removal of ocular artifact from the EEG: a review",

Neurophysiologie Clinique/Clinical Neurophysiology, Vol. 30, No. 1, pp. 5–19, 2000.

45. Hyvärinen, A., J. Karhunen and E. Oja, *Independent component analysis*, Vol. 46, John Wiley & Sons, 2004.

46. Jung, T.-P., S. Makeig, C. Humphries, T.-W. Lee, M. J. Mckeown, V. Iragui and T. J. Sejnowski, "Removing electroencephalographic artifacts by blind source separation", *Psychophysiology*, Vol. 37, No. 2, pp. 163–178, 2000.

47. Mognon, A., J. Jovicich, L. Bruzzone and M. Buiatti, "ADJUST: An automatic EEG artifact detector based on the joint use of spatial and temporal features", *Psychophysiology*, Vol. 48, No. 2, pp. 229–240, 2011.

48. Chaumon, M., D. V. Bishop and N. A. Busch, "A practical guide to the selection of independent components of the electroencephalogram for artifact correction", *Journal of neuroscience methods*, Vol. 250, pp. 47–63, 2015.

49. Bell, A. J. and T. J. Sejnowski, "An information-maximization approach to blind separation and blind deconvolution", *Neural computation*, Vol. 7, No. 6, pp. 1129–1159, 1995.

50. Huang, N. E., Z. Shen, S. R. Long, M. C. Wu, H. H. Shih, Q. Zheng, N.-C. Yen, C. C. Tung and H. H. Liu, "The empirical mode decomposition and the Hilbert spectrum for nonlinear and non-stationary time series analysis", *Proceedings of the Royal Society of London A: mathematical, physical and engineering sciences*, Vol. 454, pp. 903–995, The Royal Society, 1998.

51. Wu, Z. and N. E. Huang, "Ensemble empirical mode decomposition: a noise-assisted data analysis method", *Advances in adaptive data analysis*, Vol. 1, No. 01, pp. 1–41, 2009.

52. Delorme, A. and S. Makeig, "EEGLAB: an open source toolbox for analysis of single-trial EEG dynamics including independent component analysis", *Journal of*

neuroscience methods, Vol. 134, No. 1, pp. 9–21, 2004.

53. Scherg, M., "Fundamentals of dipole source potential analysis", *Auditory evoked magnetic fields and electric potentials. Advances in audiology*, Vol. 6, pp. 40–69, 1990.

54. Oostendorp, T. F. and A. Van Oosterom, "Source parameter estimation in inhomogeneous volume conductors of arbitrary shape", *IEEE Transactions on Biomedical Engineering*, Vol. 36, No. 3, pp. 382–391, 1989.

55. Lancaster, J. L., M. G. Woldorff, L. M. Parsons, M. Liotti, C. S. Freitas, L. Rainey, P. V. Kochunov, D. Nickerson, S. A. Mikiten and P. T. Fox, "Automated Talairach atlas labels for functional brain mapping", *Human brain mapping*, Vol. 10, No. 3, pp. 120–131, 2000.

56. Lancaster, J., L. Rainey, J. Summerlin, C. Freitas, P. Fox, A. Evans, A. Toga and J. Mazziotta, "Automated labeling of the human brain: a preliminary report on the development and evaluation of a forward-transform method", *Human brain mapping*, Vol. 5, No. 4, p. 238, 1997.

57. Newbold, P., W. Carlson and B. Thorne, "Statistics for business and economics", , 2005.

58. Coan, J. A. and J. J. Allen, "Frontal EEG asymmetry as a moderator and mediator of emotion", *Biological psychology*, Vol. 67, No. 1-2, pp. 7–50, 2004.

59. Hagemann, D., E. Naumann, J. F. Thayer and D. Bartussek, "Does resting electroencephalograph asymmetry reflect a trait? An application of latent state-trait theory.", *Journal of personality and social psychology*, Vol. 82, No. 4, p. 619, 2002.

60. Harmon-Jones, E., P. A. Gable and C. K. Peterson, "The role of asymmetric frontal cortical activity in emotion-related phenomena: A review and update", *Biological psychology*, Vol. 84, No. 3, pp. 451–462, 2010.

61. Carp, J. and R. J. Compton, "Alpha power is influenced by performance errors", *Psychophysiology*, Vol. 46, No. 2, pp. 336–343, 2009.

62. Park, J. L., M. M. Fairweather and D. I. Donaldson, "Making the case for mobile cognition: EEG and sports performance", *Neuroscience & Biobehavioral Reviews*, Vol. 52, pp. 117–130, 2015.

63. Johannesen, J. K., J. Bi, R. Jiang, J. G. Kenney and C.-M. A. Chen, "Machine learning identification of EEG features predicting working memory performance in schizophrenia and healthy adults", *Neuropsychiatric electrophysiology*, Vol. 2, No. 1, p. 3, 2016.

64. HajiHosseini, A. and C. B. Holroyd, "Reward feedback stimuli elicit high-beta EEG oscillations in human dorsolateral prefrontal cortex", *Scientific reports*, Vol. 5, p. 13021, 2015.

65. Drueke, B., L. Weichert, T. Forkmann, V. Mainz, S. Gauggel and M. Boecker, "Neural correlates of positive and negative performance feedback in younger and older adults", *Behavioral and Brain Functions*, Vol. 11, No. 1, p. 17, 2015.

66. López-Aranda, M. F., J. F. López-Téllez, I. Navarro-Lobato, M. Masmudi-Martín, A. Gutiérrez and Z. U. Khan, "Role of layer 6 of V2 visual cortex in object-recognition memory", *Science*, Vol. 325, No. 5936, pp. 87–89, 2009.

67. Picard, N. and P. L. Strick, "Imaging the premotor areas", *Current opinion in neurobiology*, Vol. 11, No. 6, pp. 663–672, 2001.

68. Allman, J. M., A. Hakeem, J. M. Erwin, E. Nimchinsky and P. Hof, "The anterior cingulate cortex: the evolution of an interface between emotion and cognition", *Annals of the New York Academy of Sciences*, Vol. 935, No. 1, pp. 107–117, 2001.

69. Carmichael, S. and J. L. Price, "Sensory and premotor connections of the orbital and medial prefrontal cortex of macaque monkeys", *Journal of Comparative Neu-*

rology, Vol. 363, No. 4, pp. 642–664, 1995.

70. Carmichael, S. and J. L. Price, "Limbic connections of the orbital and medial prefrontal cortex in macaque monkeys", *Journal of Comparative Neurology*, Vol. 363, No. 4, pp. 615–641, 1995.

71. Haber, S. N., K. Kunishio, M. Mizobuchi and E. Lynd-Balta, "The orbital and medial prefrontal circuit through the primate basal ganglia", *Journal of Neuroscience*, Vol. 15, No. 7, pp. 4851–4867, 1995.

72. Morecraft, R. J., D. W. McNeal, K. S. Stilwell-Morecraft, M. Gedney, J. Ge, C. M. Schroeder and G. W. Van Hoesen, "Amygdala interconnections with the cingulate motor cortex in the rhesus monkey", *Journal of Comparative Neurology*, Vol. 500, No. 1, pp. 134–165, 2007.

73. Öngür, D., X. An and J. Price, "Prefrontal cortical projections to the hypothalamus in macaque monkeys", *Journal of Comparative Neurology*, Vol. 401, No. 4, pp. 480–505, 1998.

74. DePasque, S. and E. Tricomi, "Effects of intrinsic motivation on feedback processing during learning", *NeuroImage*, Vol. 119, pp. 175–186, 2015.

75. Murty, V. P., K. S. LaBar and R. A. Adcock, "Distinct medial temporal networks encode surprise during motivation by reward versus punishment", *Neurobiology of learning and memory*, Vol. 134, pp. 55–64, 2016.

76. Buckholtz, J. W., C. L. Asplund, P. E. Dux, D. H. Zald, J. C. Gore, O. D. Jones and R. Marois, "The neural correlates of third-party punishment", *Neuron*, Vol. 60, No. 5, pp. 930–940, 2008.

77. Woo, Y.-k., J. Song, Y. Jiang, C. Cho, M. Bong and S.-i. Kim, "Effects of informative and confirmatory feedback on brain activation during negative feedback processing", *Frontiers in human neuroscience*, Vol. 9, p. 378, 2015.

78. Nieuwenhuis, S., H. A. Slagter, V. Geusau, N. J. Alting, D. J. Heslenfeld and C. B. Holroyd, "Knowing good from bad: differential activation of human cortical areas by positive and negative outcomes", *European Journal of Neuroscience*, Vol. 21, No. 11, pp. 3161–3168, 2005.

79. McCoy, A. N., J. C. Crowley, G. Haghighian, H. L. Dean and M. L. Platt, "Saccade reward signals in posterior cingulate cortex", *Neuron*, Vol. 40, No. 5, pp. 1031–1040, 2003.

80. Andreou, C., H. Frielinghaus, J. Rauh, M. Mußmann, S. Vauth, P. Braun, G. Leicht and C. Mulert, "Theta and high-beta networks for feedback processing: a simultaneous EEG–fMRI study in healthy male subjects", *Translational psychiatry*, Vol. 7, No. 1, p. e1016, 2017.

81. Jung, J., K. Jerbi, T. Ossandon, P. Ryvlin, J. Isnard, O. Bertrand, M. Guénot, F. Mauguière and J.-P. Lachaux, "Brain responses to success and failure: direct recordings from human cerebral cortex", *Human brain mapping*, Vol. 31, No. 8, pp. 1217–1232, 2010.

82. Rushworth, M., M. E. Walton, S. W. Kennerley and D. Bannerman, "Action sets and decisions in the medial frontal cortex", *Trends in cognitive sciences*, Vol. 8, No. 9, pp. 410–417, 2004.

83. Gehring, W. J. and A. R. Willoughby, "The medial frontal cortex and the rapid processing of monetary gains and losses", *Science*, Vol. 295, No. 5563, pp. 2279–2282, 2002.

84. Miltner, W. H., C. H. Braun and M. G. Coles, "Event-related brain potentials following incorrect feedback in a time-estimation task: evidence for a "generic" neural system for error detection", *Journal of cognitive neuroscience*, Vol. 9, No. 6, pp. 788–798, 1997.

85. Ruchsow, M., J. Grothe, M. Spitzer and M. Kiefer, "Human anterior cingulate

cortex is activated by negative feedback: evidence from event-related potentials in a guessing task", *Neuroscience letters*, Vol. 325, No. 3, pp. 203–206, 2002.